SLEEP, 2022, 1–21

https://doi.org/10.1093/sleep/zsac135
Advance Access Publication Date: 7 June 2022
Original Article

ORIGINAL ARTICLE

Inflammation, tau pathology, and synaptic integrity associated with sleep spindles and memory prior to β-amyloid positivity

Bryce A. Mander[1,2,3,*], Abhishek Dave[1,3], Kitty K. Lui[1,4], Katherine E. Sprecher[5,6,7], Destiny Berisha[8], Miranda G. Chappel-Farley[2,8], Ivy Y. Chen[1], Brady A. Riedner[9], Margo Heston[6,7], Ivonne Suridjan[10], Gwendlyn Kollmorgen[11], Henrik Zetterberg[12,13,14,15], Kaj Blennow[12,13], Cynthia M. Carlsson[7,16,17], Ozioma C. Okonkwo[7,16,17], Sanjay Asthana[7,16,17], Sterling C. Johnson[7,16,17], Barbara B. Bendlin[7,16,17] and Ruth M. Benca[1,2,5,8,9,18,*]

[1]Department of Psychiatry and Human Behavior, University of California, Irvine, CA, USA, [2]Center for the Neurobiology of Learning and Memory, University of California, Irvine, CA, USA, [3]Department of Cognitive Sciences, University of California, Irvine, CA, USA, [4]San Diego State University/University of California San Diego, Joint Doctoral Program in Clinical Psychology, San Diego, CA, USA, [5]Neuroscience Training Program, University of Wisconsin-Madison, Madison, WI, USA, [6]Department of Medicine, University of Wisconsin-Madison, Madison, WI, USA, [7]Wisconsin Alzheimer's Disease Research Center, University of Wisconsin-Madison, Madison, WI, USA, [8]Department of Neurobiology and Behavior, University of California, Irvine, CA, USA, [9]Department of Psychiatry, University of Wisconsin-Madison, Madison, WI, USA, [10]Roche Diagnostics International Ltd, Rotkreuz, Switzerland, [11]Roche Diagnostics GmbH, Penzberg, Germany, [12]Institute of Neuroscience and Physiology, University of Gothenburg, Gothenburg, Sweden, [13]Clinical Neurochemistry Laboratory, Sahlgrenska University Hospital, Mölndal, Sweden, [14]Department of Neurodegenerative Disease, UCL Institute of Neurology, Queen Square, London, UK, [15]UK Dementia Research Institute at UCL, London, UK, [16]Wisconsin Alzheimer's Institute, Madison, WI, USA, [17]Geriatric Research Education and Clinical Center, Wm. S. Middleton Veterans Hospital, Madison, WI, USA and [18]Department of Psychiatry and Behavioral Medicine, Wake Forest University, Winston-Salem, NC, USA

*Corresponding author. Ruth M. Benca, Department of Psychiatry and Behavioral Medicine, Wake Forest University, Winston Salem, NC, 27103, USA. Email: rbenca@wakehealth.edu; Bryce A. Mander, Department of Psychiatry and Human Behavior, University of California, Irvine, CA 92617, USA. Email: bmander@uci.edu.

Abstract

Study Objectives: Fast frequency sleep spindles are reduced in aging and Alzheimer's disease (AD), but the mechanisms and functional relevance of these deficits remain unclear. The study objective was to identify AD biomarkers associated with fast sleep spindle deficits in cognitively unimpaired older adults at risk for AD.

Methods: Fifty-eight cognitively unimpaired, β-amyloid-negative, older adults (mean ± SD; 61.4 ± 6.3 years, 38 female) enriched with parental history of AD (77.6%) and apolipoprotein E (APOE) ε4 positivity (25.9%) completed the study. Cerebrospinal fluid (CSF) biomarkers of central nervous system inflammation, β-amyloid and tau proteins, and neurodegeneration were combined with polysomnography (PSG) using high-density electroencephalography and assessment of overnight memory retention. Parallelized serial mediation models were used to assess indirect effects of age on fast frequency (13 to <16Hz) sleep spindle measures through these AD biomarkers.

Results: Glial activation was associated with prefrontal fast frequency sleep spindle expression deficits. While adjusting for sex, APOE ε4 genotype, apnea–hypopnea index, and time between CSF sampling and sleep study, serial mediation models detected indirect effects of age on fast sleep spindle expression through microglial activation markers and then tau phosphorylation and synaptic degeneration markers. Sleep spindle expression at these electrodes was also associated with overnight memory retention in multiple regression models adjusting for covariates.

Conclusions: These findings point toward microglia dysfunction as associated with tau phosphorylation, synaptic loss, sleep spindle deficits, and memory impairment even prior to β-amyloid positivity, thus offering a promising candidate therapeutic target to arrest cognitive decline associated with aging and AD.

Submitted: 5 September, 2021; **Revised:** 17 May, 2022

Statement of Significance

Aging and Alzheimer's disease disrupt sleep spindle expression, but the mechanisms and functional relevance of these sleep spindle deficits remain unclear. Here, we examined multiple facets of central nervous system inflammation, a factor driving Alzheimer's disease pathogenesis, and related them to Alzheimer's disease biomarkers, neuronal integrity, sleep spindle expression, and memory in cognitively unimpaired, β-amyloid-negative, older adults at increased Alzheimer's disease risk. We found that (i) sleep spindle associations were mediated through associations of microglia activation with phosphorylated tau proteins and synaptic integrity and (ii) sleep spindles were associated with sleep-dependent memory. These findings identify microglia dysfunction as a potential trigger of tau-dependent sleep spindle and memory deficits even prior to β-amyloid positivity; offering a promising candidate therapeutic target to arrest the cognitive decline.

Graphical Abstract

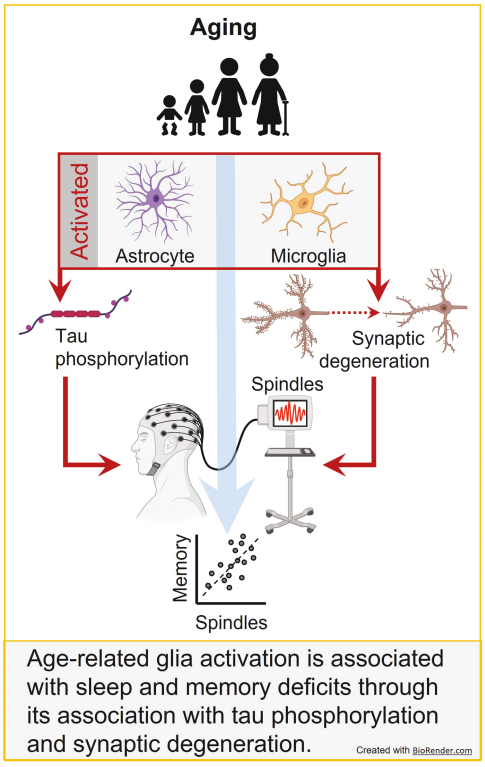

Key words: Alzheimer's disease; sleep spindles; tau phosphorylation; inflammation; neurodegeneration; memory

Introduction

Aging and Alzheimer's disease (AD) are associated with deposition of neuropathology, reductions in neuronal integrity, neural network dysfunction, and central nervous system (CNS) inflammation [1–3]. Local expression of sleep oscillations associated with neuroplasticity and memory consolidation, particularly nonrapid eye movement (NREM) cortico-thalamic fast frequency (13–16 Hz) sleep spindles, are also disrupted by aging and AD pathophysiology [4, 5], yet the mechanisms underlying these sleep spindle deficits and their functional significance in the context of cognitive decline are not completely known. Inflammation is hypothesized to be a core mechanism linking aging to sleep disturbance, neuronal degeneration and dysfunction, pathogenesis of neurodegenerative disease, and cognitive decline [1, 6, 7]. While these measures have been examined in relation to aging and dementia in isolation [8–19], their interrelationships are unknown, especially as they relate to fast frequency sleep spindle oscillations that support neuroplasticity and memory. Furthermore, it is unknown which specific markers of CNS inflammation, AD pathophysiology, and neuronal integrity drive these relationships. Addressing these knowledge gaps is critical for elucidating therapeutic targets responsible for cognitive decline and dementia risk in later life.

NREM sleep spindles, particularly those expressed in higher frequencies (13 to <16 Hz), are brain oscillations that critically support neuroplasticity, learning, and memory consolidation [4, 5, 20–24]. These brain oscillations, generated in the reticular nucleus of the thalamus and expressed in cortico-thalamic loops [25], can facilitate the induction of long-term potentiation or depression at synapses [24], and organize hippocampal ripple-induced replay of memories in support of memory consolidation in the cortex [21]. Blocking their expression impairs memory consolidation [21], whereas enhancing NREM sleep spindles, particularly those expressed at higher frequencies [14–16 Hz], enhances memory consolidation [22].

Both aging and AD disrupt local expression of fast frequency sleep spindles [4, 5, 11, 13, 26–31], and these sleep spindle

deficits have been associated with reduced grey matter volume [9], white matter integrity [27], and accumulation of tau proteins and pathology [13, 18, 32] in cognitively unimpaired older adults. Moreover, fast-frequency sleep spindle deficits are magnified in patients with mild cognitive impairment (MCI) and AD [11, 29, 31]. Loss of fast frequency sleep spindles in aging and AD is associated with impaired hippocampal function, memory encoding, long-term memory retention, and cognition [8, 9, 26, 27, 33–36], suggesting that fast frequency sleep spindle deficits contribute to cognitive impairment in aging and AD. However, it remains unclear whether local sleep spindle deficits are apparent in individuals at risk for AD prior to β-amyloid (Aβ) plaque deposition, whether they impact sleep-dependent cognition, and which AD pathophysiological mechanisms are associated with them.

Aging is associated with increased chronic low-grade inflammation, termed "inflammaging" [37], which may be involved in dementia [1, 37]. A large body of work implicates inflammation as a core mechanism driving AD progression [38, 39]. Current evidence indicates that Aβ pathology can disrupt astrocyte and microglia function, which then promotes the accumulation and spread of tau pathology, triggering neurodegeneration and cognitive impairment [38, 39]. However, inflammaging can also promote AD pathophysiology prior to Aβ plaque deposition [40]. Since deficits in sleep spindle expression have been associated with markers of AD pathology and neurodegeneration in cognitively unimpaired older adults [9, 13, 18, 27], it is possible that inflammation may disrupt sleep spindle expression through its impact on these processes even prior to MCI or AD dementia diagnosis. If the local expression of memory-relevant sleep oscillations is impacted by mechanisms of CNS inflammaging, this could provide a novel mechanism underlying associations between chronic inflammation and memory impairment [7, 41–43], and may reveal a novel pathway for inflammaging to contribute to cognitive decline. CNS inflammation has been implicated in a number of the pathological changes observed in aging and AD [7, 38, 39, 44, 45], and there is an extensive literature on the bidirectional interactions between global sleep measures and inflammation [6]. However, CNS inflammation could also trigger changes in brain structure and AD biomarkers, resulting in local disruptions in sleep oscillations and related memory impairment. To date, no study has directly addressed this possibility.

We targeted these critical knowledge gaps by combining examination of cerebrospinal fluid (CSF) biomarkers of astrocyte and microglial activation (Glial fibrillary acidic protein [GFAP], calcium-binding proteins [S100B], chitinase-3-like protein [YKL-40], soluble triggering receptor expressed on myeloid cell 2 [sTREM2]), AD-related proteins ($Aβ_{40}$, $Aβ_{42}$, $Aβ_{42/40}$, total tau [t-tau], phos-phorylated tau [p-tau]) and neuronal and synaptic degeneration (α-synuclein, neurogranin, neurofilament light chain [NfL]) with polysomnography (PSG) using high-density electroencephalography (hdEEG; 256 channels) and assessment of overnight memory retention in cognitively unimpaired, β-amyloid and tau-negative older adults (based on CSF thresholds) enriched for AD risk (*APOE* ε4-positive genotype and/or parental history of AD). Using serial parallel mediation modeling, we tested the hypothesis that CNS inflammaging is associated with local sleep spindle deficits and impaired sleep-dependent memory through associations with markers of AD-related proteins and neuronal integrity. We further characterized whether these effects were driven primarily by astrocytic or microglial activation, β-amyloid or tau proteins, and/or synaptic or axonal degeneration, thus elucidating specific biological mechanisms associating aging with sleep-dependent memory deficits among individuals at risk for AD.

Methods

Participants and study design

About Fifty-eight clinically normal and cognitively unimpaired middle-aged and older adults (mean ± *SD*; 61.4 ± 6.3 years, 38 female) were recruited from the Wisconsin Alzheimer's Disease Research Center clinical core (Table 1). The sample was enriched with AD risk factors compared with the general population (77.6% parental history of AD, 25.9% *APOE* ε4-positive genotype). Cohort participants were recruited from the community via advertisements and word of mouth, and were free of history of any significant neurological, psychiatric, or medical conditions and related treatments impacting cognition, the ability to comply with the study protocol, or impacting sleep or CSF measurements. Medications known to affect sleep and sleep electroencephalography (EEG), including antipsychotic medications, nonselective serotonin reuptake inhibitors (SSRIs) antidepressants, neuroleptics, chronic anxiolytics, sedative-hypnotics, and stimulants, were exclusionary. Participants underwent comprehensive cognitive testing, medical history assessment, and CSF sampling at the University of Wisconsin-Madison. Cognitive testing covered the domains of declarative and semantic memory, attention, executive function, language, and visuospatial processing using the National Alzheimer's Coordinating Center Uniform Data Set neuropsychological battery version 3 and additional assessments [46]. Cognitive status was determined using standard criteria and adjudicated by a consensus conference [47, 48]. Participants performed within standardized norms of the cognitively normal UDS cohort on all neuropsychological tests (Supplementary Table S1) [46]. Polysomnography (PSG) was performed as part of a separate substudy in participants who did not currently use therapy for sleep-disordered breathing (e.g. CPAP) and did not have any major neurological, medical, or psychiatric illness. While the presence of obstructive sleep apnea (OSA), defined as having an apnea–hypopnea index (AHI) > 5 [49], was not exclusionary in this study, AHI was included as a covariate in relevant analyses to adjust for the influence of OSA. When CSF was available from multiple time points, the data from the CSF sample collected closest to the polysomnography were used (on average the time between assessments was 2.1 ± 2.1 years). All participants provided informed consent, and protocols were approved by the Institutional Review Board of the University of Wisconsin-Madison.

Polysomnography

Sleep was evaluated in all participants using standard polysomnography (PSG) including electrooculogram (EOG), submental electromyogram (EMG), electrocardiogram (ECG), bilateral tibial EMG, respiratory inductance plethysmography, pulse oximetry and a position sensor using a customized Alice 5 System (Philips Respironics, Murrysville, PA). Simultaneously, high-density electroencephalography (hdEEG) was recorded

at 500 Hz from 256 channels with vertex referencing using a NetAmps 300 amplifier and NetStation software (Electrical Geodesics Inc., Eugene, OR). Sleep staging was performed using 6 hdEEG channels located at approximately 10–20 locations (F3, F4, C3, C4, O1, and O2), re-referenced to the contralateral mastoid. A registered sleep technologist scored sleep following AASM scoring guidelines [49, 50] using Alice Sleepware (Philips Respironics, Murrysville, PA). A physician (author R.B.) certified in Sleep Medicine by the American Board of Medical Specialties reviewed the scoring and assessed the presence and severity of sleep disorders, including sleep apnea. Multiple established sleep architecture variables were computed, including total recording time (TRT; duration between lights off and lights on), total sleep time (TST; total duration of all sleep stages between lights off and lights on), sleep latency (SL; time to first scored epoch of sleep), sleep efficiency (SE; percent of TRT spent asleep), wake after sleep onset (WASO; duration of wake time following sleep onset), percent of TST spent in stages N1, N2, N3, and R, AHI (number of apnea and hypopnea events per hour), respiratory disturbance index (RDI; number of apnea, hypopnea, and respiratory-related arousals per hour), and the periodic leg movements during sleep index (PLMSI; number of PLMs per hour). Mean values across the participant cohort for each of these variables are presented in Table 1.

Table 1. Participant characteristics (n = 58)

	Mean (±SD)
Demographics	
Age at PSG (years)	61.4 ± 6.3
Age at CSF sample (years)	59.3 ± 6.1
Interval from CSF sample to PSG (years)	2.1 ± 2.1
Female (*n*;%)	38; 65.5
APOE ε4-positivegenotype (*n*, %)	15; 25.9
Parental history of AD positive (*n*, %)	45; 77.6
Geriatric depression scale	0.6 ± 1.1
Education (years)	16.5 ± 2.1
Sleep architecture	
Time in bed (minutes)	446.5 ± 57.8
Total sleep time (minutes)	347.8 ± 71.3
Sleep onset latency (minutes)	19.1 ± 23.0
Sleep efficiency (%)	78.0 ± 13.2
Wake after sleep onset (minutes)	79.6 ± 51.9
Stage N1 (%)	9.0 ± 9.6
Stage N2 (%)	58.6 ± 11.0
Stage N3 (%)	14.3 ± 11.0
Stage REM (%)	17.9 ± 6.0
Apnea–hypopnea index (AHI; number/hour)	7.9 ± 12.5
AHI < 5 (*n*, %)	34; 58.6
AHI 5–<15 (*n*, %)	15; 25.9
AHI 15—<30 (*n*, %)	5; 8.6
AHI 30 + (*n* ,%)	4; 6.9
Respiratory disturbance index (number/hour)	15.6 ± 16.5
Periodic leg movements index (number/hour)	16.8 ± 19.0
Cerebrospinal fluid biomarkers	
GFAP (ng/L)	8.18 ± 2.7
S100B (ng/mL)	1.19 ± 0.27
YKL-40 (pg/mL)	132.4 ± 44.3
sTREM2 (pg/mL)	7.8 ± 2.2
$A\beta_{42/40}$	0.069 ± 0.010
$A\beta_{40}$ (pg/mL)	13514 ± 3994
$A\beta_{42}$ (pg/mL)	933 ± 321
t-tau (pg/mL)	179.2 ± 69.3
p-tau (pg/mL)	15.0 ± 4.3
α-synuclein (pg/mL)	135.6 ± 62.3
neurogranin (pg/mL)	677.0 ± 245.5
NfL (pg/mL)	92.1 ± 119.3

AD denotes Alzheimer's disease, APOE denotes apolipoprotein E, Aβ denotes β-amyloid, CSF denotes cerebrospinal fluid, GFAP denotes Glial fibrillary acidic protein, NfL denotes neurofilament light chain protein, PSG denotes polysomnography, p-tau denotes phosphorylated tau, S100B denotes calcium binding protein B, sTREM2 denotes soluble triggering receptor expressed on myeloid cell 2, t-tau denotes total tau, YKL-40 denotes chitinase-3-like protein.

EEG spectral analysis

Data preprocessing, including semiautomated artifact rejection [51–53], and analyses of sleep data focusing on NREM stages (N2 and N3) were performed using custom MATLAB (Mathworks, Inc., R2017b) scripts with the EEGLAB toolbox (https://sccn.ucsd.edu/eeglab/index.php), similar to previously described [54]. In short, EEG data were notch filtered in the 59.5–60.5 Hz frequency range, and then bandpass-filtered in the 0.3–55 Hz frequency range. A 5500-point Hamming windowed sinc Finite Impulse Response filter was used in both instances. The 50 outermost electrodes were excluded from further analyses, due to recurring physiological artifacts at these locations across subjects. The remaining 206 electrodes were average referenced and manually inspected for persistent, long-duration noise to delete compromised electrodes. Thereafter, data corresponding to NREM stages were extracted from these electrodes and concatenated into a combined matrix. Subsequently, a three-stage semi-automated artifact rejection process was used to reject short durations of widespread noise and consistently noisy EEG derivations [51–53]. First, epochs marked with arousals were removed from analysis. Second, an automated 99.8 percentile threshold on broadband power spectral density was used to eliminate high-powered artifact bursts in the remaining epochs. Third, visual inspection was used to flag and reject remaining short-duration artifacts and any remaining noisy, artifact-filled electrodes. Last, the data for deleted EEG derivations were reconstructed from vicinal electrodes using spherical spline interpolation that yielded clean EEG data from NREM sleep epochs for all 58 subjects [55, 56]. Spectral analyses of cleaned data were conducted with a Fast Fourier Transform approach, leveraging the multitaper method to generate estimates of absolute and relative spectral power in the 0.5–40 Hz range for each electrode. These analyses relied on the use of 11 discrete prolate spheroidal sequence (DPSS) tapers and were parameterized with a bandwidth of 0.25 Hz, zero-order padding, and a 30 s input window, sliding every 5 s. From these estimates, 30 s windows of median absolute spectral power were computed across NREM epochs for each of the 1294 frequency bins within the overall spectrogram, at each electrode. Mean absolute power was then computed across NREM epochs by averaging within the frequency bins corresponding to each canonical frequency band (i.e. slow oscillation: 0.5–<1 Hz, delta: 1–<4.5 Hz, theta: 4.5–<7.5 Hz, alpha: 7.5–<11 Hz, slow sigma: 11–<13 Hz, fast sigma: 13–<16 Hz, beta: 16–<28 Hz, and gamma: 28–40 Hz), and were used for further analyses. An a priori focus on absolute fast sigma activity was implemented for analyses, given our focus on sleep spindle-related measures and the importance of fast frequency sleep spindles for aging, AD, and memory consolidation [11, 22, 30]. All spectral analyses were conducted with the Chronux v2.12 toolbox (http://chronux.org) for MATLAB [57–59].

Parameterizing NREM power spectra by fitting oscillations and one over F (FOOOF)

The FOOOF approach (specparam, version 1.0.0) [60] was leveraged to analyze EEG data to quantify and distinguish between pure oscillatory activity and background aperiodic activity which is ascribed to putative neural noise. While traditional measurements of absolute and relative spectral power conflate contributions of the periodic and aperiodic components of the signal spectrum [61], the FOOOF approach disentangles the two and quantifies their parameters separately (Supplementary Figures S1 and S2). This approach was implemented to isolate differences in oscillatory activity localized to the fast sigma [13–<16 Hz] frequency range from global differences in aperiodic, generalized power across individuals (Supplementary Figure S1A). The FOOOF algorithm operates iteratively on inputs of power spectral density by utilizing a combination of linear regressions in log-frequency—log-power space and gaussians that are fit to peaks in the oscillatory residual (represented as aperiodic fits iteratively subtracted first from the original power spectrum, and subsequently from each iteration of the parameterized spectrum). This results in an optimized spectral curve that contains separable components of isolated oscillatory and aperiodic activity. The area under the curve of the oscillatory residual in the fast sigma frequency range [13–<16 Hz] thus represents spectral power associated with canonically defined fast sleep spindles (Supplementary Figure S1B). Spectral parameterization was carried out for each subject using the cluster average of absolute power spectral densities obtained from the multitaper method described above at 11 fronto-central channels showing significant overlapping associations between absolute fast sigma activity and markers of CNS inflammation, AD-related proteins, measures of synaptic and axonal integrity, and overnight memory retention. The FOOOF algorithm was implemented with the following parameters (input frequency range = 0.5–40 Hz, maximum peaks = 9, peak width = 0.5–4 Hz, minimum absolute peak height = 0.03 log (μV [2]/Hz), minimum relative peak height threshold = 1.2 standard deviations above the aperiodic fit) using a modified version of the MATLAB wrapper for the FOOOF package for Python (version 3.8.3). The algorithm recommends the use of a knee frequency for aperiodic fits when the range of input frequencies exceeds ~40 Hz, and when there are characteristic timescales in the underlying data, resulting in a bend ("knee") in the power spectrum in the log–log space of power and frequency [60, 62]. Animal studies have shown that distinct vigilance states, including NREM sleep, exhibit unique electrophysiological timescales [63]. This analysis therefore operationalized the FOOOF algorithm with a knee frequency parameter. FOOOF algorithm outputs included both parameterized spectra and the parameters used to generate aperiodic and oscillatory fits. For this study, these parameters included (1) fast sigma oscillatory activity, (2) the aperiodic 1/*f* exponent, (3) the aperiodic offset, and (4) the aperiodic knee frequency (Supplementary Figure S2). The area under the parameterized oscillatory residual from 13 to <16 Hz was used to capture canonically true fast spindle oscillatory activity. The knee frequency denotes an exception to the scale-free or fractal nature generally ascribed to the 1/*f* aperiodic component, wherein a bend in the aperiodic spectrum occurs after a region with relatively shallow or flat slope within the spectrum, representing a characteristic timescale in underlying neural data. The exponent of the linear, scale-free 1/*f* component corresponds to the slope of the aperiodic fit beyond the knee frequency and is associated with the excitatory/inhibitory tone in neuronal populations, with steeper slopes reflecting reduced excitatory:inhibitory ratio [64]. The aperiodic offset is associated with broadband power in the spectrum, and is tied to background spiking activity in neuronal populations in intracranial local field potential studies [62, 65]. Analyses in this study focused on relating fast sigma oscillatory activity, the aperiodic 1/*f* exponent, and the aperiodic offset to age, CNS inflammation measures, AD-related proteins, neuronal integrity markers, and measures of overnight memory retention.

EEG sleep spindle analysis

Sleep spindles were detected and quantified using the validated A7 algorithm relying on default threshold settings, as described previously [66]. In short, sleep spindles were detected in artifact-free, concatenated signals in N2 and N3 staged epochs in the same 206 hdEEG channels used for spectral analysis. The A7 algorithm uses a combination of log-transformed absolute power, Z-normalized log-transformed relative power, and the correlation and covariance between the original N2 and N3 time series and the bandpass filtered signal in the range 11–<16 Hz. These four parameters are all computed in 0.3 s sliding time windows with a 0.1 s step size. Each parameter is associated with a detection threshold, and all four detection thresholds must be exceeded simultaneously for underlying data to be classified as belonging to a sleep spindle. Targeted spindle durations were in the range 0.3–2.5 s. Outputs generated from the detection algorithm included sleep spindle count, sleep spindle density (spindle count divided by minutes of artifact-free N2/N3 sleep), and sleep spindle durations. Sleep spindle durations were then averaged across channels to yield mean spindle duration for each of the 206 electrodes.

To additionally classify detected sleep spindles as either fast (13–<16 Hz) or slow (11–<13 Hz) spindles, previously detected spindles were extracted individually from cleaned NREM data that were filtered in the 11–<16 Hz range, for each subject at each electrode. Every sleep spindle then underwent an FFT-based spectral power calculation, using a rectangular window with zero-padding to the nearest power of 2. The peak frequency in each spindle segment was identified as the frequency corresponding to the highest value of spectral power. Sleep spindles were classified as either fast or slow based on their calculated peak frequencies, with peak frequencies below 13 Hz corresponding to slow sleep spindles and peak frequencies at or above 13 Hz corresponding to fast sleep spindles. Subsequently, the mean fast and slow sleep spindle durations were calculated separately for each subject at each EEG derivation by averaging the durations of individual fast and slow sleep spindles. Fast and slow sleep spindle densities were calculated by dividing the count of fast and slow sleep spindles respectively by minutes of artifact-free N2 and N3 sleep stages. Fast sleep spindle density and mean fast sleep spindle duration were then leveraged in subsequent correlations and regression analyses as primary sleep spindle measures. Sleep spindle density and mean sleep spindle duration for total and slow sleep spindles were included in Supplementary Information as secondary analyses for completeness.

CSF collection and analysis

Cerebrospinal fluid (CSF) was collected in the morning following an 8–12-hour fast. Typically, a Sprotte 25- or 24-gauge spinal needle was used to perform a lumbar puncture at L3/4 or L4/5. Approximately 22 mL of CSF was obtained via gentle extraction into polypropylene syringes, then gently mixed to remove gradient effect and centrifuged for 10 min at 2000 g. Supernatants were frozen in 0.5 mL aliquots in polypropylene tubes and stored at –80°C within 30 min of collection. Assays were conducted by board-certified laboratory technicians blinded to participant clinical characteristics.

The NeuroToolKit (Roche Diagnostics International Ltd, Rotkreuz, Switzerland) was implemented to assess levels of multiple fluid biomarkers in human CSF and comprises a panel of automated CSF immunoassays [67]. The NeuroToolKit robust prototype assays are for investigational purposes and are not approved for clinical use. All samples were assayed using the same batch of reagents under strict quality control procedures at the Clinical Neurochemistry Laboratory, University of Gothenburg. Elecsys Aβ(1–42) CSF, Elecsys Phospho-Tau (181P; p-tau) CSF and Elecsys Total-Tau (t-tau) CSF, Aβ(1-40) and S100 calcium-binding protein B (S100B) immunoassays were performed on a cobas e 601 analyzer (Roche Diagnostics International Ltd), while neurogranin, neurofilament light protein (NfL), α-synuclein, glial fibrillary acidic protein (GFAP), chitinase-3-like protein 1(YKL-40), and soluble triggering receptor expressed on myeloid cells 2 (sTREM2) were performed on a cobas e 411 analyzer (Roche Diagnostics International Ltd).

Each of these CSF fluid biomarkers targeted specific aspects of CNS inflammation, AD-related proteins, and neuronal integrity. While GFAP and S100B are both implicated in activated astrocytes, YKL-40 is a glycoprotein expressed in both astrocytes and microglia, and sTREM2 is considered a marker of microglia activation [67]. In terms of AD-related proteins, $A\beta_{40}$ and $A\beta_{42}$ were assessed, and $A\beta_{42}$ was also expressed in ratio to $A\beta_{40}$ (the more abundant, nontoxic species) to assess the pathologic fragment (Aβ42) while accounting for individual differences in overall amyloid production. Both t-tau and p-tau reflect total tau protein levels and levels of tau phosphorylated at threonine-181, respectively, with the latter being more reflective of risk for developing neurofibrillary tangles [67]. Amyloid and tau pathology positivity thresholds were derived from receiver operating characteristic (ROC) analyses on a larger sample, as described previously [67], with Aβ positivity being indicated from an $A\beta_{42/40}$ ratio < 0.046 and tau positivity being indicated from p-tau > 24.8 pg/mL. Only one participant showed an $A\beta_{42/40}$ ratio < 0.046 (0.041) and none exhibited tau positivity based on these thresholds, thus Aβ and tau measures were not directly quantifying AD pathologies but instead assessing AD-related proteins that may precede the later development of measurable pathologies such as Aβ plaque deposition and development of neurofibrillary tangles [68]. Though slight decreases in CSF α-synuclein levels in Parkinson's disease (PD) have been associated with deposition within Lewy bodies, increases of this presynaptic marker in CSF likely tracks synaptic degeneration in non-PD populations [67]. Neurogranin, a post-synaptic protein, is highly associated with α-synuclein in this sample ($r^2 = 0.67$, $p = .0002$) and also tracks synaptic degeneration, while NfL is a known marker of axonal degeneration [67]. CSF Aβ, t-tau, p-tau, and S100 values were missing for one participant, and values for another subject were excluded as outliers for t-tau (>5 standard deviations from mean) and NfL (>7 standard deviations from mean).

Word-pairs memory task

A word-pairs task targeting overnight episodic memory retention, shown in previous studies to be sensitive to sleep-dependent memory consolidation in young adults and individuals with MCI [31, 69–71], was implemented in the current study. The task was administered using E-Prime 2.0 software (Psychology Software Tools, Pittsburgh, PA), and had three phases (i.e. encoding, immediate recall, and delayed recall). The encoding phase occurred in the evening prior to sleep onset. During this phase, 88 word-pairs were presented sequentially for four seconds, with each pair presented with one word shown above the other in the center of a computer monitor. Participants were instructed to learn the word-pairs for later recall. To avoid primacy and recency effects, the first and last four word-pairs were not included in either recall phase. The immediate recall phase occurred after completion of the encoding phase, and the delayed recall phase occurred in the morning, one hour after sleep offset. During both recall phases, one word was presented in the middle of the screen, and participants were instructed to type in the corresponding word from the pairs they had just studied. The order of word-pairs was randomized across phases and subjects, and their responses were self-paced. To minimize bias due to experimenter feedback, participants were seated with the experimenter out of view, and typed responses into the computer. Errors that were clearly typographic rather than a failure of recall (e.g. forg instead of frog) were later corrected by the experimenter offline, prior to data analysis. During the immediate recall phase, after all 80 word-pairs were presented, a feedback screen displayed their accuracy (i.e. percent correct). Encoding and immediate recall phases were repeated until > 60% accuracy was achieved, and the final immediate recall phase was used for analysis. The delayed recall phase was conducted only once and feedback was not given, regardless of accuracy. Performance accuracy during immediate and delayed recall phases were calculated as the proportion of trials correctly answered. The difference in performance across test phases, representing a measure of overnight episodic memory retention, was derived in two ways. An absolute difference in performance accuracy (defined as post-sleep—pre-sleep performance accuracy) and a proportion in the difference in performance accuracy (defined as [post-sleep—pre-sleep performance accuracy]/pre-sleep performance accuracy) were calculated and used in analyses. Word-pairs task memory performance measures were missing for four participants, thus all analyses with memory data included 54 participants.

Statistical analysis

Normality of variables was assessed using the Shapiro–Wilk test, and data were transformed to support parametric statistical approaches. Specifically, CSF measures of sTREM2, $A\beta_{40}$, $A\beta_{42}$, t-tau, p-tau, neurogranin, NFL were logarithmic transformed (base 10). A reciprocal transformation was used for α-synuclein since logarithmic transformation failed to adequately transform the data. Thus, all true relationships with α-synuclein should be considered the opposite sign as presented in the current

report (i.e. a positive association presented with the reciprocal should be interpreted to represent a negative association with CSF α-synuclein levels). A cube root transformation was used to minimize negative skew in memory performance variables, and significant associations using Pearson's *r* were further confirmed with nonparametric Kendall's tau-b correlations. All other variables examined were normally distributed.

Pearson's *r* values were computed at each electrode across topography for associations between spectral power, sleep spindle density and duration for total, fast, and slow sleep spindles, and age, CSF fluid biomarkers, and overnight change in word-pairs memory performance. The Threshold-Free Cluster Enhancement (TFCE) procedure (5000 permutations, alpha = 0.05, extent parameter: 0.5, height parameter: 2.0) was used to correct for multiple comparisons across topography [72–74]. Absolute spectral power from resulting clusters of significant electrodes following TFCE correction were extracted, averaged, and then utilized in follow-up multiple linear regression models examining relationships between spectral power, sleep spindle density and duration, and age, CSF fluid biomarkers, and overnight change in word-pairs memory performance while adjusting for confounding covariates.

Multiple linear regression models were used to examine associations between age, CSF fluid biomarkers, spectral power across frequencies, sleep spindle density and mean sleep spindle duration during NREM sleep for total, fast, and slow sleep spindles, and overnight change in word-pairs memory performance. All multiple linear regression models relied on a 5000-sample bootstrapping procedure to generate bias-corrected and accelerated 95% confidence intervals [75]. In models predicting CSF variables, age at CSF collection, AHI, *APOE* ε4 genotype, and sex were used as covariates. In models predicting spectral estimates, sleep spindle density, and mean sleep spindle duration during sleep, age at CSF collection, time difference between CSF collection and sleep study, AHI, *APOE* ε4 genotype, and sex were included as covariates. In models predicting memory performance, age at sleep study, *APOE* ε4 genotype, and sex were included as covariates.

Mediation analyses were performed using the Process Macro v3.5 for SPSS [76], implementing model 80 to assess indirect effects in a combined parallel and serial mediation framework. Within this template, age at CSF collection was used as the predictor (X), while the outcome (Y) was mean absolute fast sigma power [13–<16 Hz], fast sigma oscillatory activity, sleep spindle density or mean sleep spindle duration druring NREM sleep for total, fast, and slow sleep spindles at the time of the sleep study. CSF markers of astrocyte and microglia activation (i.e. GFAP, S100B, YKL-40, log sTREM2) were harnessed as the parallel mediators (M1, M2, M3, and M4, respectively). A unique serial mediator (M5) followed M1-M4 in the model to examine indirect effects of inflammation on fast sleep spindle measures, with M5 defined separately in five different models as CSF markers of AD-related proteins and neuronal integrity (i.e. log t-tau, log p-tau, 1/α-synucleiun, log neurogranin, log NfL). The Huber–White method was used to account for heteroscedasticity in the data, and 10 000-sample bootstrapping was used to generate upper and lower limits for confidence intervals for indirect effects to minimize distributional assumptions in smaller sample sizes [77]. When 95% confidence intervals did not include 0, the indirect effect was considered significant (α = 0.05). All mediation analyses included sex, *APOE* ε4 genotype, AHI, and time between CSF collection and sleep study as covariates.

For the above analyses, TFCE correction for multiple comparisons was conducted using a custom MATLAB script, as described previously [72–74]. All other analyses were conducted in SPSS v26.0 (IBM SPSS Statistics, Inc., Chicago, IL).

Data visualization

For visualization purposes, only electrodes falling within a plotting radius of 0.56 (using the topoplot function in EEGlab) from the center of the scalp were presented in all topographical plots. A perceptually uniform, colorblind-accessible colormap (plasma; https://bids.github.io/colormap/) was used to depict the strength of correlational findings between mean power in canonical frequency bands at these electrodes and both biological and behavioral variables of interest.

RESULTS

Participant characteristics

Subjects were middle-aged to older adults (61.4 ± 6.3 years [range: 48–80 years]), ~66% female, and considered cognitively unimpaired based on standard criteria and adjudicated by consensus conference (Table 1 and Supplementary Table S1). The sample was enriched for AD risk (77.6% parental history of AD, 25.9% *APOE* ε4-positive genotype). On the basis of the previously derived cutoffs [67], all participants were tau pathology negative, and all but one were β-amyloid pathology negative. Neither AHI nor periodic leg movements index during sleep (PLMSI) significantly predicted any of the CSF, sleep, or cognitive variables described below (all $r^2 < 0.063$, $p > .065$).

Age associations with CNS inflammation, AD-related proteins, neuronal integrity, and local sleep

We first examined associations between age and CSF measures and three measures of sleep spindle expression: absolute fast frequency [13–<16 Hz] sigma activity, fast sleep spindle density, and mean fast sleep spindle duration. Associations with sleep spindle density and duration for total and slow sleep spindles and absolute power in other frequency bands during NREM sleep were also explored. Multiple regression models adjusting for AHI, sex, and *APOE* ε4 genotype indicated that increasing age was significantly associated with higher levels of astrocyte and microglia activation:GFAP ($b = 0.254$, $p = .0002$), YKL-40 ($b = 3.972$, $p = .0002$), and log sTREM2 ($b = 0.0086$, $p = .0006$); as well as AD-related proteins: log t-tau ($b = 0.009$, $p = .0014$), log p-tau ($b = 0.008$, $p = .0046$); and axonal and synaptic degeneration: 1/α-synuclein ($b = -0.0002$, $p = .001$), and log NFL ($b = 0.015$, $p = .0002$). Full statistical details are presented in Supplementary Table S2. Thus, age was associated with increased levels of astrocyte and microglial activation, as well as tau, α-synuclein, and NfL.

Age was significantly associated with widespread reduction in sigma power, particularly in higher frequencies (13–<16 Hz; Figures 1A and Supplementary Figure S1). Peak negative associations between age and absolute fast sigma activity were detected following threshold-free cluster enhancement (TFCE) correction for multiple comparisons over anterior frontal and parietal electroencephalography (EEG) derivations. We next averaged fast sigma activity across 52 EEG derivations exhibiting

TFCE-corrected significant associations with age and included this fast sigma activity average in a multiple regression model adjusting for sex, AHI, and *APOE* ε4 genotype. Age remained a significant predictor of fast sigma activity ($b = –0.008$, $p = .040$) following adjustment for covariates. Due to concerns about generalized reductions in EEG amplitude confounding this association, follow-up analyses orthogonalized the power–frequency spectrum from this TFCE-corrected cluster into three components: (i) fast sigma oscillatory activity, (ii) the aperiodic 1/*f* exponent, and (iii) the aperiodic power offset. Fast sigma oscillatory activity was significantly associated with age ($r = –0.41$, $p = .001$), while both the aperiodic 1/*f* exponent ($r = 0.18$, $p = .182$) and power offset ($r = 0.06$, $p = .649$) were not. Age was also significantly associated with topographically similar reductions in fast sleep spindle density and mean fast sleep spindle duration (Figure 1B and C). Fast sleep spindle density ($b = –0.044$, $p = .013$), mean fast sleep spindle duration ($b = –0.007$, $p = .002$), total sleep spindle density ($b = –0.072$, $p = .012$), and mean total sleep spindle duration ($b = –0.0007$, $p = .004$) averaged across TFCE-corrected significant associations were also significantly predicted by age in similar multiple regression models (Supplementary Table S2, Figures S4–S7). In contrast, we did not detect significant negative associations between age and slow sleep spindle density or absolute spectral power at any derivation in any other frequency bands following TFCE correction in this sample (Supplementary Figures S3—S7). These findings confirm that age, at least across the range of the study cohort, was associated with reductions in fronto-parietal sleep spindle expression.

CNS inflammation and AD-related proteins, neuronal integrity, and local sleep

We next sought to determine whether CNS inflammation was associated with AD-related proteins, neuronal degeneration, and local deficits in sleep spindle measures. Multiple regression models, adjusting for AHI, age at CSF sampling, sex, and *APOE* ε4 genotype indicated that GFAP, YKL-40, S100B, and log sTREM2 all significantly predicted log t-tau (for GFAP $b = 0.013$, $p = .027$; for S100B $b = 0.175$, $p = .007$; for YKL-40 $b = 0.002$, $p = .0002$; for log sTREM2 $b = 0.675$, $p = .0002$), 1/α-synuclein (for GFAP $b = –0.00038$, $p = .016$; for S100B $b = –0.003$, $p = .011$; for YKL-40 $b = –0.000041$, $p = .0002$; for log sTREM2 $b = –0.015$, $p = .0002$), and log NfL (for GFAP $b = 0.020$, $p = .018$; for S100B $b = 0.143$, $p = .041$; for YKL-40 $b = .001$, $p = .001$; for log sTREM2 $b = 0.722$, $p = .0002$). Only YKL-40, S100B, and log sTREM2 significantly predicted log $A\beta_{40}$ (for S100B $b = 0.163$, $p = .006$; for YKL-40 $b = 0.002$, $p = .0002$; for log sTREM2 $b = 0.623$, $p = .0002$), log p-tau (for S100B $b = 0.181$, $p = .006$; for YKL-40 $b = 0.002$, $p = .0002$; for log sTREM2 $b = 0.731$, $p = .0002$), and log neurogranin (for S100B $b = 0.170$, $p = .035$; for YKL-40 $b = 0.003$, $p = .0002$; for log sTREM2 $b = 0.838$, $p = .0004$), although GFAP trended towards significance for log p-tau ($b = 0.011$, $p = .072$). Only YKL-40 ($b = 0.003$, $p = .0002$) and log sTREM2 ($b = 0.617$, $p = .0004$) significantly predicted log $A\beta_{42}$. Full statistical details are presented in Supplementary Table S3. CSF biomarkers of astrocyte and microglia activation were thus consistently associated with multiple markers of Aβ proteins, tau proteins and markers of neuronal integrity.

With respect to associations between measures of CNS inflammation and sleep spindle expression, TFCE-corrected significant associations were detected between fast sigma activity and GFAP, YKL-40, S100B and log sTREM2 over fronto-central EEG derivations (Figure 2A—D). A group of 11 electrodes showed TFCE corrected associations with fast sigma activity that overlapped for GFAP, YKL-40, S100B, and log sTREM2. Fast sigma activity was averaged across these derivations and included in multiple regression models predicting fast sigma activity while adjusting for age at CSF sampling, sex, AHI, time between CSF sampling and sleep study, and *APOE* ε4 genotype. Of these CNS inflammation markers, only YKL-40 remained a significant predictor of fast sigma activity ($b = –0.001$, $p = .035$) following adjustment for covariates; S100B ($b = –0.141$, $p = .064$) and log sTREM2 ($b = –0.255$, $p = .093$) trended toward significance. Addressing concerns regarding generalized reductions in EEG amplitude, fast sigma oscillatory activity was significantly associated with GFAP ($r = –0.28$, $p = 0.036$), S100B ($r = –0.32$, $p = .015$), and YKL-40 ($r = –0.32$, $p = .016$), with log sTREM2 trending to significance ($r = –0.23$, $p = .080$). Neither the aperiodic 1/*f* exponent nor the aperiodic offset was significantly associated with any CNS inflammation measure (all $r^2 < 0.063$, all $p > .05$). Similar topographic patterns of associations were observed between all glial activation markers and fast sleep spindle density and mean fast sleep spindle duration measures, with associations between fast sleep spindle density and GFAP, S100B, YKL-40, and log sTREM2 reaching TFCE-corrected significance over fronto-central derivations, and TFCE-corrected associations between mean fast sleep spindle duration and GFAP, YKL-40, and log

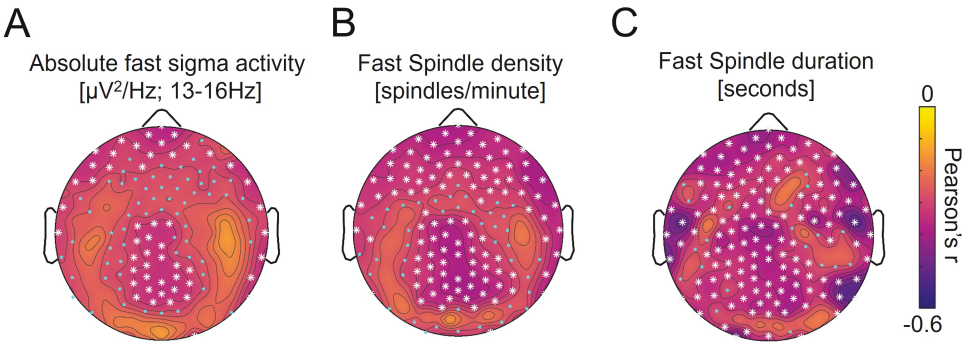

Figure 1. Topographic plots of associations between age and fast sleep spindle measures, including (a) absolute power in the fast sigma frequency range [13–<16 Hz], (b) fast sleep spindle density, and (c) mean fast sleep spindle duration during nonrapid eye movement (NREM) sleep across electroencephalography (EEG) derivations. Cooler colors represent more negative associations, while warmer colors reflect more positive associations. Cyan dots indicate EEG derivations exhibiting significant associations ($p < .05$ uncorrected), while white asterisks denote significant associations following correction for multiple comparisons across the entire EEG array ($p < .05$ threshold-free cluster enhancement [TFCE] corrected [72–74]).

sTREM2 also peaking over fronto-central derivations (Figure 2). Similar to findings with fast sigma activity, multiple regression models revealed that mean fast sleep spindle duration was associated with log sTREM2 ($b = -0.31$, $p = .025$), total sleep spindle density was associated with S100B ($b = -1.6$, $p = .044$), and total sleep spindle duration was associated with YKL-40 ($b = -0.001$, $p = .041$) and log sTREM2 ($b = -0.32$, $p = .043$) after adjusting for covariates (Supplementary Table S3, Figures S4—S7). The only TFCE-corrected significant negative association between glial activation markers and absolute power in other frequency bands was between S100B and slow sigma power over frontal derivations (Supplementary Figures S8—S11). These findings indicate that measures of astrocytic and microglial activation were associated with deficits in sleep spindle expression over fronto-central EEG derivations.

AD-related proteins and neuronal integrity and local sleep

Markers of CNS inflammaging were consistently associated with markers of Aβ and tau proteins, neuronal degeneration, and local deficits in sleep spindle expression. We next examined whether AD-related proteins were associated with markers of neuronal integrity and local expression of sleep spindles. Multiple regression models, adjusting for age at CSF sampling, AHI, sex, and *APOE* ε4 genotype indicated that log $A\beta_{40}$, log $A\beta_{42}$, log t-tau, and log p-tau all significantly predicted 1/α-synuclein (for log $A\beta_{40}$ $b = -0.016$, $p = .0002$, for log $A\beta_{42}$ $b = -0.01$, $p = .0002$, for log t-tau $b = -0.018$, $p = .0002$; for log p-tau $b = -0.019$, $p = .0002$), log neurogranin (for log $A\beta_{40}$ $b = 1.14$, $p = .0002$, for log $A\beta_{42}$ $b = 0.79$, $p = .0002$, for log t-tau $b = 1.290$, $p = .0002$; for log p-tau $b = 1.267$, $p = .0002$), and log NfL (for log $A\beta_{40}$ $b = 0.486$, $p = .001$, for log $A\beta_{42}$ $b = -0.287$, $p = .009$, for log t-tau $b = 0.574$, $p = .0002$; for log p-tau $b = 0.519$, $p = .006$). No significant effects were detected for $A\beta_{42/40}$ predicting log t-tau, log p-tau, log NFL, log neurogranin, or 1/α-synuclein (all $p > .35$). Full statistical details are presented in Supplementary Table S4.

Both t-tau and p-tau predicted sleep spindle expression, as TFCE-corrected significant associations with fast sigma activity, fast sleep spindle density, and mean fast sleep spindle duration were detected globally, peaking over fronto-central EEG derivations (Figure 3). Notably, the same group of 11 electrodes described above showed TFCE corrected associations with fast sigma activity that overlapped for GFAP, YKL-40, S100B, log sTREM2, log t-tau, and log p-tau. Fast sigma activity was averaged across these derivations and included in multiple regression models predicting fast sigma activity while adjusting for age at CSF sampling, sex, AHI, time between CSF sampling and sleep study, and *APOE* ε4 genotype. Both tau protein markers

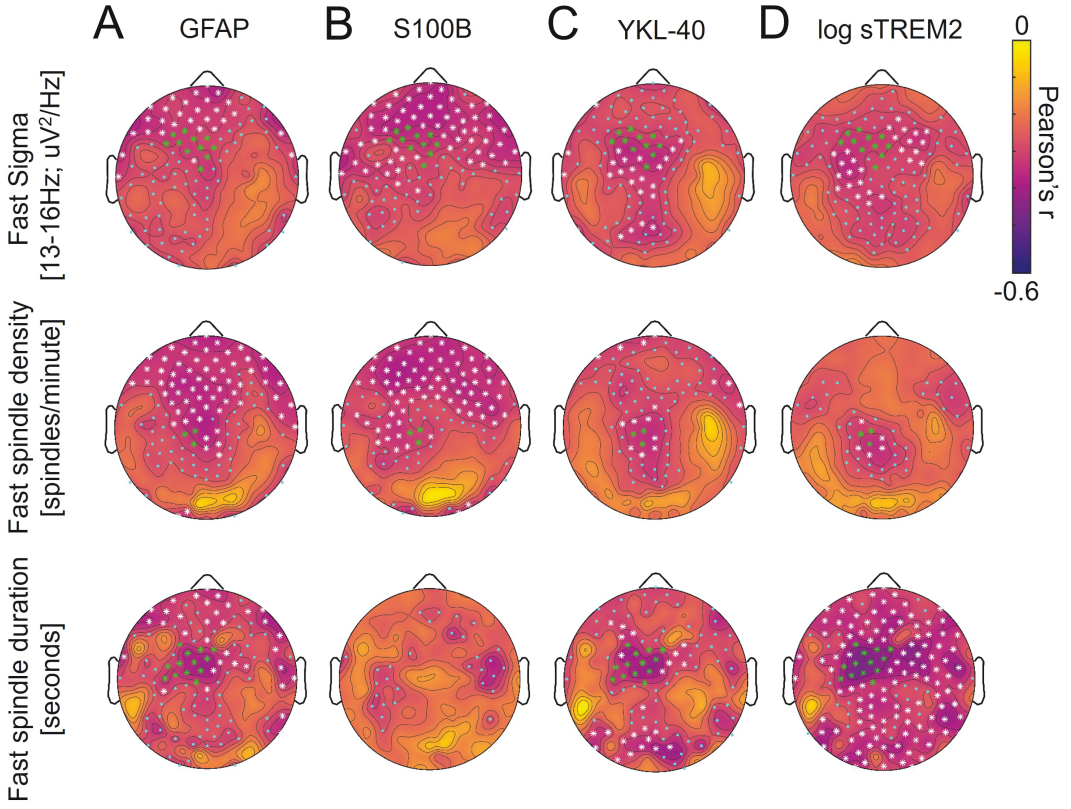

Figure 2. Topographic plots of associations between cerebrospinal fluid (CSF) (a) glial fibrillary acidic protein (GFAP), (b) calcium binding protein B (S100B), (c) chitinase-3-like protein (YKL-40), and (d) log soluble triggering receptor expressed on myeloid cell 2 (sTREM2) levels and absolute power in the fast sigma frequency range [13 to <16 Hz] (top panel), fast sleep spindle density (middle panel), and mean fast sleep spindle duration (bottom panel) during nonrapid eye movement (NREM) sleep across electroencephalography (EEG) derivations. In the top and middle panels, green asterisks denote EEG derivations where threshold-free cluster enhancement (TFCE) corrected significant associations were detected across assessed markers of glial fibrillary acidic protein [GFAP], calcium binding protein B [S100B], chitinase-3-like protein [YKL-40], log soluble triggering receptor expressed on myeloid cell 2 [sTREM2], log total tau [t-tau], log phosphorylated tau [p-tau], 1/α-synuclein, log neurogranin, and log neurofilament light chain protein [NfL] (11 derivations for fast sigma activity and 3 derivations for fast sleep spindle density). In the bottom panel, green asterisks denote EEG derivations where TFCE-corrected significant associations were detected across assessed markers of GFAP, YKL-40, log sTREM2, log t-tau, log p-tau, 1/α-synuclein, log neurogranin, and log neurofilament light chain protein [NfL] (13 derivations).

remained significant predictors of fast sigma activity (for log t-tau $b = -0.477$, $p = .004$; for log p-tau $b = -0.499$, $p = .001$) following adjustment for covariates. Fast sigma oscillatory activity averaged at this 11-electrode cluster was also significantly associated with log $A\beta_{40}$ ($r = -0.30$, $p = .024$), log p-tau ($r = -0.48$, $p = .0002$), and log t-tau ($r = -0.44$, $p = .001$), while the aperiodic $1/f$ exponent was not (all $r^2 < 0.012$, all $p > .41$). In addition to the fast sigma oscillatory activity, the aperiodic offset was independently associated with log p-tau ($r = -0.27$, $p = .047$), and trended towards significance with log $A\beta_{40}$ ($r = -0.23$, $p = .092$) and log t-tau ($r = -0.26$, $p = .056$). The pattern of associations with tau protein markers was similar for fast sleep spindle density and mean fast sleep spindle duration, and both log t-tau (for fast sleep spindle density $b = -4.3$, $p = .023$; for mean fast sleep spindle duration $b = -0.40$, $p = .009$) and log p-tau (for fast sleep spindle density $b = -4.6$, $p = .008$; for mean fast sleep spindle duration $b = -0.45$, $p = .003$) remained significant predictors after adjusting for covariates. Associations between log t-tau and total sleep spindle density, mean total sleep spindle duration, and mean slow sleep spindle duration were detected following TFCE correction, whereas associations between log p-tau and total sleep spindle density, mean total sleep spindle duration, slow sleep spindle density, and mean slow sleep spindle duration were also detected (Supplementary Figures S4—S7). In all cases, these associations remained significant following adjustment of covariates (all $p \leq .016$). CSF $A\beta_{42/40}$ was positively associated with absolute fast sigma activity, fast sleep spindle duration, total sleep spindle density, mean total sleep spindle duration, slow sleep spindle density, and slow sleep spindle duration, particularly over frontal and posterior occipito-temporal derivations (Figures 3 and Supplementary Figures S4—S7), but the association between $A\beta_{42/40}$ and absolute sigma activity was more robust in the slow sigma frequency range (11–<13 Hz; Supplementary Figure S12). Averaged across the TFCE-corrected significant electrodes, $A\beta_{42/40}$ remained a significant predictor of slow (80 electrodes; $b = 10.545$, $p = .023$) and fast (26 electrodes; $b = 3.919$, $p = .021$) sigma activity following adjustment for age at CSF sampling, sex, AHI, *APOE* ε4 genotype, and time between CSF sampling and sleep study. Associations between $A\beta_{42/40}$ and mean fast sleep spindle duration, total sleep spindle density, mean total sleep spindle duration, slow sleep spindle density, and mean slow sleep spindle duration were observed over frontal derivations following TFCE correction for multiple comparisons (Figures 3 and Supplementary Figures S4—S7), and associations with total sleep spindle density ($b = 39.6$, $p = .037$) and slow sleep spindle density ($b = 34.6$, $p = .024$) remained significant following adjustment for covariates. Associations between log $A\beta_{40}$ and fast sigma activity were also present over frontal derivations (Figure 3B, Supplementary Table S4). However, in a model incorporating log p-tau, log $A\beta_{40}$ was no longer significant ($p = .066$) while log p-tau remained significant (Adjusted $r^2 = 0.28$, $p = .001$, log p-tau $p = .002$). Following TFCE correction, the only significant associations between $A\beta_{42/40}$, log $A\beta_{40}$, log $A\beta_{42}$, log p-tau, or log t-tau and absolute spectral power across other frequencies bands was observed between tau measures and power in the slow sigma and beta frequency bands (Supplementary Figures S12—S15). Collectively, these findings indicate that CSF levels of AD-related proteins were consistently associated with deficits in sleep spindle expression.

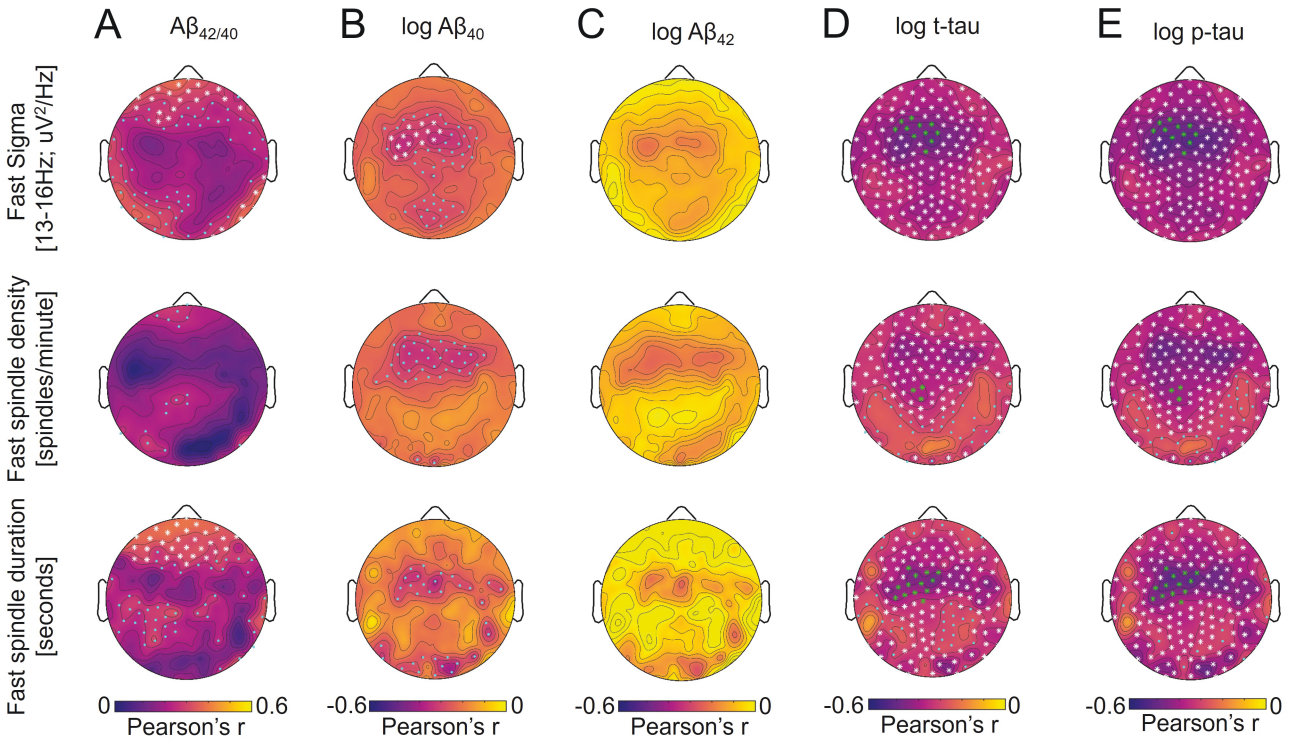

Figure 3. Topographic plots of associations between cerebrospinal fluid (CSF) (a) ratio of β-amyloid 42 to β-amyloid 40 ($A\beta_{42/40}$), (b) log Aβ40, (c) log Aβ42, (d) log total tau (t-tau), and (e) log phosphorylated tau (p-tau) and absolute power in the fast sigma frequency range [13 to <16 Hz] (top panel), fast sleep spindle density (middle panel), and mean fast sleep spindle duration (bottom panel) during NREM sleep across electroencephalography (EEG) derivations.

Neuronal integrity and local sleep

All three markers of neuronal integrity (α-synuclein, neurogranin, NfL) exhibited robust associations with absolute fast sigma activity, fast sleep spindle density, and mean fast sleep spindle duration following TFCE correction (Figure 4, Supplementary Table S5). These associations were largely global, with peak effects over fronto-parietal derivations, but were specific to faster frequencies for α-synuclein and neurogranin while being seen across a broader frequency range for NfL (Supplementary Figures S16—S18). The same group of 11 electrodes described above also showed TFCE corrected associations with fast sigma activity that overlapped for GFAP, YKL-40, S100B, log sTREM2, log t-tau, log p-tau, 1/α-synuclein, log neurogranin, and log NfL. Absolute fast sigma activity was averaged across these derivations and included in multiple regression models predicting fast sigma activity while adjusting for sex, AHI, *APOE* ε4 genotype, age at CSF sampling, and time between CSF sampling and sleep study. Both 1/α-synuclein and log neurogranin remained significant predictors of fast sigma activity (for 1/α-synuclein $b = 22.404$, $p = .001$; for log neurogranin $b = –0.324$, $p = .004$), whereas log NfL ($b = –0.249$, $p = .058$) trended to significance following adjustment for covariates. Fast sigma oscillatory activity averaged at this 11-electrode cluster was also significantly associated with 1/α-synuclein ($r = 0.46$, $p = .0003$) and log neurogranin ($r = –0.35$, $p = .008$), whereas the aperiodic 1/f exponent and aperiodic offset were not (all $r^2 < 0.07$, all $p > .05$). Neither the fast sigma oscillatory activity ($r = –0.21$, $p = .121$) nor the aperiodic 1/*f* exponent ($r = –0.08$, $p = .555$) was significantly associated with log NfL, though the aperiodic offset was associated ($r = –0.26$, $p = .050$), indicating that spectral power associations with log NfL may be driven by broadband power differences among individuals. The topographic pattern of associations with neuronal integrity markers was similar for fast sleep spindle density and mean fast sleep spindle duration, and 1/α-synuclein (for fast sleep spindle density $b = 271.8$, $p = .001$; for mean fast sleep spindle duration $b = 22.2$, $p = .001$) and log neurogranin (for fast sleep spindle density $b = –2.6$, $p = .038$; for mean fast sleep spindle duration $b = –0.30$, $p = .007$) remained significant predictors after adjusting for covariates. Associations did not remain significant for log NfL (for fast sleep spindle density $b = –1.9$, $p = .252$; for mean fast sleep spindle density $b = –0.20$, $p = .058$) after adjusting for covariates. TFCE corrected associations were also detected between 1/α-synuclein, log neurogranin, and log NfL and total sleep spindle density, mean total sleep spindle duration, slow sleep spindle density, and mean slow sleep spindle duration (Supplementary Figures S2—S5). Following adjustment for covariates, associations with all these sleep spindle measures remained significant for 1/α-synuclein and log neurogranin (all $p \leq .013$) but only mean total sleep spindle duration remained a significant predictor of log NfL ($b = –0.29$, $p = .024$).

All neuronal integrity markers exhibited TFCE-corrected significant associations with spectral power in other frequency bands, with 1/α-synuclein being negatively associated with slow sigma, beta, and gamma frequency power, log neurogranin being negatively associated with slow sigma and beta power, and log NfL being associated with spectral power across nearly all frequency bands (Supplementary Figures S16—S18).

These analyses indicate that multiple markers of neuronal integrity, particularly those more sensitive to synaptic degeneration (α-synuclein, neurogranin), were significantly associated with deficits in sleep spindle expression during NREM sleep, with peak associations occurring at fronto-central EEG derivations also showing peak associations with CNS inflammation and tau proteins. Full statistical details are presented in Supplementary Table S5.

Tau proteins and neural integrity mediate associations between inflammation and sleep

Peak associations with sleep spindle measures were remarkably consistent topographically across CSF fluid biomarkers of CNS inflammation, tau proteins, and neuronal integrity, indicating the possibility of interrelationships among all these variables. To integrate the above findings, serial mediation models were conducted in the SPSS Process Macro v3.5, using model 80 to compute indirect effects in a parallelized serial mediation framework (Figure 5A) [76]. Mediation analyses incorporated sex, *APOE* ε4 genotype, AHI, and time between CSF sampling and sleep study as covariates. These models characterized the presence of statistically significant serial mediations, with all markers of astrocyte and microglia activation (GFAP, S100B, YKL-40, log sTREM2) independently mediating the effects of age on markers of tau proteins (log t-tau, log p-tau) and neuronal integrity (1/α-synuclein, log neurogranin, log NfL), with each in turn mediating the effects of GFAP, S100B, YKL-40, and log sTREM2 on sleep spindle measures (fast sigma activity, fast sigma oscillatory activity, fast sleep spindle density, mean fast sleep spindle duration). As secondary analyses, indirect effects on total sleep spindle density, mean total sleep spindle duration, slow sleep spindle density, and mean slow sleep spindle duration were also explored. For fast sigma activity, significant serial mediation effects were detected using 95% confidence intervals through YKL-40 and then log t-tau (indirect effect = –0.0031, CI: –0.0073 to –0.00004), log p-tau (indirect effect = –0.0036, CI: –0.0077 to –0.0037), and 1/α-synuclein (indirect effect = –0.0021, CI: –0.0047 to –0.0001), and through log sTREM2 and then log p-tau (–0.0021, CI: –0.0049 to –0.0001) and 1/α-synuclein (–0.0020, CI: –0.005 to –0.00004; Figure 5B, Supplementary Tables S6—S10). Mediation models examining indirect effects on fast sigma oscillatory activity confirmed these results on fast sigma activity, with indirect effects detected through YKL-40 and then log t-tau (indirect effect = 0.034, CI: –0.091 to –0.0004), log p-tau (indirect effect = –0.040, CI: –0.092 to –0.005), and 1/α-synuclein (indirect effect = –0.025, CI: –0.060 to –0.003), and through log sTREM2 and then log p-tau (indirect effect = –0.023, CI: –0.052 to –0.002), and 1/α-synuclein (indirect effect = –0.023, CI: –0.059 to –0.002, Supplementary Tables S11—S15). Similar indirect effects were also identified for fast sleep spindle density and mean fast sleep spindle duration, as well as total sleep spindle density and mean total sleep spindle duration (Figure 5B, Supplementary Tables S16—S35). More specifically, significant serial mediation effects were detected through YKL-40 and then log p-tau for fast sleep spindle duration (indirect effect = –0.0034, CI: –0.0073 to –0.0002), 1/α-synuclein for fast sleep spindle density (indirect effect = –0.029, CI: –0.062 to –0.004), mean fast sleep spindle duration (indirect effect = –0.0022, CI: –0.0048 to –0.0002), total sleep spindle density (indirect effect = –0.030, CI: –0.063 to –0.005), and mean total sleep spindle duration (indirect effect = –0.00193, CI: –0.00425 to –0.00017). Indirect effects were also detected through log sTREM2 and then log p-tau for fast

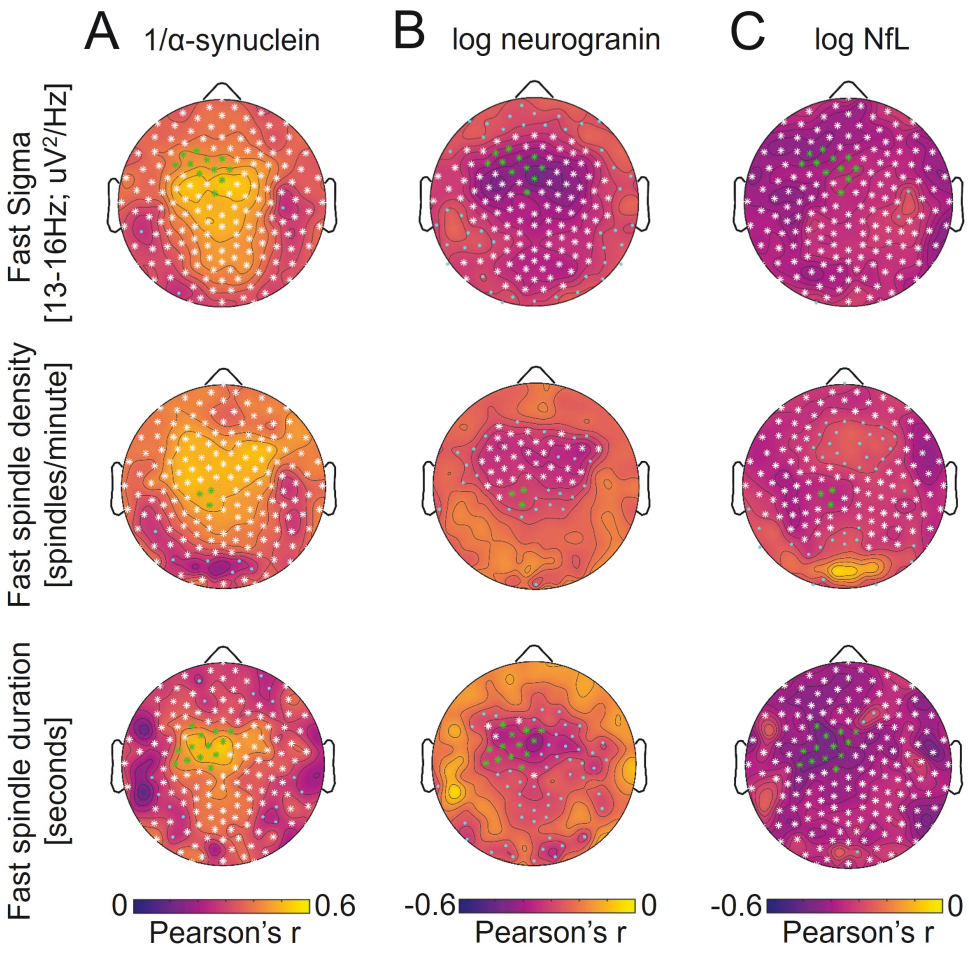

Figure 4. Topographic plots of associations between cerebrospinal fluid (CSF) (a) 1/α-synuclein, (b) log neurogranin, and (c) log neurofilament light-chain protein (NfL) and absolute power in the fast sigma frequency range [13 to <16 Hz] (top panel), fast sleep spindle density (middle panel), and mean fast sleep spindle duration (bottom panel) during NREM sleep across electroencephalography (EEG) derivations.

sleep spindle duration (indirect effect = –0.0019, CI: –0.0047 to –0.0002) and 1/α-synuclein for fast sleep spindle density (indirect effect = –0.027, CI: –0.065 to –0.003), mean fast sleep spindle duration (indirect effect = –0.021, CI: –0.005 to –0.00015), total sleep spindle density (–0.028, CI: –0.069 to –0.003) and mean total sleep spindle duration (–0.00182, CI: –0.00456 to –0.00008). No other significant indirect effects were detected. Collectively, these findings suggest that age-related deficits in sleep spindle expression, particularly in faster frequency ranges, are more specifically associated with the effects of microglia on tau proteins and synaptic integrity.

Association between local sleep and overnight memory retention

We finally examined whether deficits in sleep spindle expression were associated with memory impairment. Overnight word-pairs memory retention was quantified as absolute change in accuracy and proportion of change in accuracy between pre-sleep and post-sleep testing sessions of the word pairs task (WPT), with values cube root transformed to minimize negative skewness. These measures exhibited strong TFCE-corrected correlations over frontal, central, and parietal derivations with mean absolute fast sigma power, total sleep spindle density, slow sleep spindle density, and mean sleep spindle duration for total, fast, and slow sleep spindles (Figure 6AC). Nonparametric Kendall's tau-b confirmed these associations with absolute fast sigma activity at 11 EEG derivations with TFCE significance overlapping with GFAP, YKL-40, log sTREM2, log t-tau, log p-tau, 1/α-synuclein, log neurogranin, log NfL, S100B, as well as absolute (Kendall's tau-*b* = 0.23, *p* = .019) and proportional (Kendall's tau-*b* = 0.22, *p* = .0.019) overnight change in word-pairs memory. Fast sigma oscillatory activity at the 11-electrode cluster (for absolute Kendall's tau-*b* = 0.24, *p* = .013; for proportional Kendall's tau-*b* = 0.23, *p* = .013) was also significantly associated with overnight change in word-pairs memory, while neither the aperiodic 1/*f* exponent (for absolute Kendall's tau-*b* = 0.14, *p* = .146; for proportional Kendall's tau-*b* = 0.15, *p* = .122) nor the aperiodic offset (for absolute Kendall's tau-*b* = 0.13, *p* = .178; for proportional Kendall's tau-*b* = 0.12, *p* = .218) were significant predictors of memory performance. While no TFCE-corrected significant associations were detected between fast sleep spindle density and overnight memory retention (Figure 6B C), associations were confirmed between fast sleep spindle density at EEG derivations with TFCE significance overlapping with all inflammation, tau proteins, and synaptic integrity markers and absolute (Kendall's tau-*b* = 0.29, *p* = .003) and proportional (Kendall's tau-*b* = 0.28, *p* = .003) overnight change in word-pairs memory. Associations

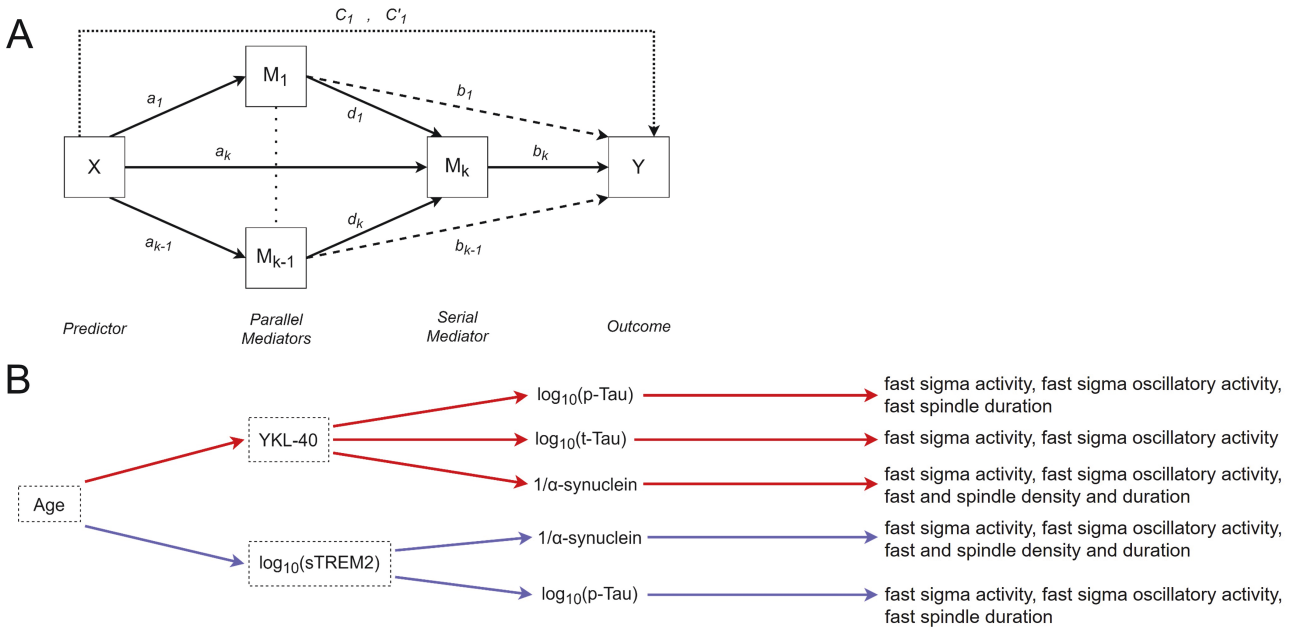

Figure 5. (a) Schematic representation of SPSS Process Macro v3.5 model 80 [76] implemented to examine combined parallel and serial mediation linking age to fast sigma activity through cerebrospinal fluid (CSF) glial fibrillary acidic protein (GFAP), calcium binding protein B (S100B), chitinase-3-like protein (YKL-40), and log soluble triggering receptor expressed on myeloid cell 2 (sTREM2) levels, respectively, and then through CSF log total tau (t-tau), log phosphorylated tau (p-tau), 1/α-synuclein, log neurogranin, and log neurofilament light chain protein (NfL) levels, comprising five separate serial mediation models. Lowercase letters a–d reflect regression coefficients corresponding to each path within the mediation model, with a_1—a_4 indicating the effect of age on inflammation markers, a_5 indicating the effect of age on markers of Alzheimer's disease (AD)-related proteins or synaptic integrity, b_1—b_4 indicating the effect of inflammation markers on sleep spindle measures in the cluster of 11 overlapping electrodes, b_5 indicating the effect of AD-related proteins or synaptic integrity on fast sigma activity, c_1 and $c_{1'}$ reflecting the total effect and direct effect of age on fast sigma activity after adjusting for mediators, and d_1—d_4 reflecting the effect of inflammation markers on AD-related proteins or synaptic integrity. (b) Schematic representation of all significant serial mediation paths linking age to sleep spindle measures (fast sigma activity [13 to <16 Hz], fast sigma oscillatory activity, fast sleep spindle density, mean fast sleep spindle duration, total sleep spindle density, and total mean sleep spindle duration) during nonrapid eye movement (NREM) sleep (Supplementary Tables S6—S35). No paths are shown for GFAP or S100B because no significant paths through these inflammation markers were detected. Significant paths through YKL-40 and log p-tau, log t-tau, and 1/α-synuclein are denoted in red, and significant paths through log sTREM2 and log p-tau and 1/α-synuclein are denoted in blue.

were also confirmed between mean fast sleep spindle duration at EEG derivations with TFCE significance overlapping with GFAP, YKL-40, log sTREM2, log t-tau, log p-tau, 1/α-synuclein, log neurogranin, log NfL, and absolute (Kendall's tau-b = 0.27, p = .005) and proportional (Kendall's tau-b = 0.26, p = .006) overnight change in word-pairs memory. Significant associations were also detected for total sleep spindle density (for absolute Kendall's tau-b = 0.28, p = .005; for proportional Kendall's tau-b = 0.26, p = .006), total sleep spindle duration (for absolute Kendall's tau-b = 0.25, p = .009; for proportional Kendall's tau-b = 0.24, p = .011), slow sleep spindle density (for absolute Kendall's tau-b = 0.23, p = .011; for proportional Kendall's tau-b = 0.24, p = .013) and mean slow sleep spindle duration (for absolute Kendall's tau-b = 0.28, p = .004; for proportional Kendall's tau-b = 0.26, p = .006). Last, memory measures were also significantly associated with absolute delta activity, theta activity, slow sigma activity, and beta activity following TFCE correction (Supplementary Figures S19–S20, Table S36).

Multiple linear regressions were employed to assess whether sleep spindle measures at electrodes showing associations with inflammation, AD-related proteins, and neuronal integrity markers significantly predicted both absolute and proportion overnight change in memory performance on the WPT. While memory measures were not significantly associated with age (all r^2 < 0.05, p > .14) or AHI (all r^2 < 0.001, p > .88), nor differed by sex (all p > .61) or APOE ε4 genotype (all p > .66), multiple regression models included an average of fast sigma activity, fast sigma oscillatory activity, fast sleep spindle duration, total sleep spindle density, mean total sleep spindle duration, slow sleep spindle density, or slow sleep spindle duration at TFCE-corrected clusters, age at PSG study, *APOE* ε4 genotype, and sex as covariates predicting word-pairs memory. Mean absolute fast sigma power remained a significant predictor of both absolute (b = 0.435, p = .009) and proportion (b = 0.483, p = .008) overnight change in WPT memory performance (Figure 6A–C). Fast sleep spindle density, mean fast sleep spindle duration, total sleep spindle density, mean total sleep spindle duration, slow sleep spindle density, and mean slow sleep spindle duration also all remained significant predictors of absolute (for fast sleep spindle density b = 0.03, p = .051; for mean fast sleep spindle duration b = 0.36, p = .035; for total sleep spindle density b = .035, p = .004; for mean total sleep spindle duration b = 0.46, p = .003; for slow sleep spindle density b = 0.04, p = .006; for mean slow sleep spindle duration b = 0.29, p = .043) and/or proportion (for fast sleep spindle density b = 0.03, p = .032; for mean fast sleep spindle duration b = 0.40, p = .034; for total sleep spindle density b = 0.04, p = .002; for mean total sleep spindle duration b = 0.52, p = .003; for slow sleep spindle density b = 0.05, p = .003; for mean slow sleep spindle duration b = 0.33, p = .048) overnight change in WPT memory performance. These findings support the hypothesis that CNS inflammaging, tau proteins, and synaptic degeneration may impact memory retention in older adults, in part,

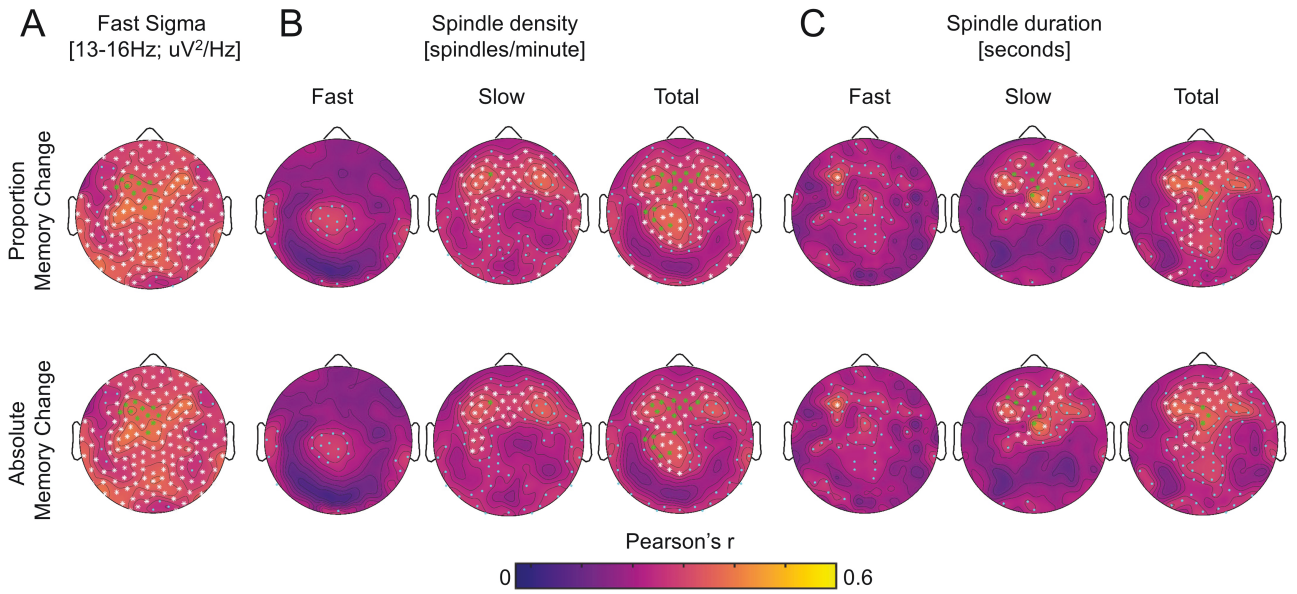

Figure 6. Topographic plots of associations between cube root of proportion (top panel) overnight memory change [(post-sleep memory—pre-sleep memory)/pre-sleep memory] and absolute (bottom panel) overnight memory change [post-sleep memory—pre-sleep memory] on the word pairs task and (a) absolute power in the fast sigma frequency range [13 to <16 Hz], (b) sleep spindle density for total spindles, fast spindles, and slow spindles, and (c) mean sleep spindle duration for total spindles, fast spindles, and slow spindles during NREM sleep across electroencephalography (EEG) derivations.

through their disruption of sleep spindle-dependent mechanisms supporting overnight memory consolidation.

Discussion

These findings demonstrate that, even prior to β-amyloid pathology positivity, inflammation in the human brain was associated with tau phosphorylation and synaptic degeneration-associated sleep spindle and memory deficits in cognitively unimpaired older adults at risk for AD. More specifically, increased microglia activation, through its association with increased levels of phosphorylated tau and synaptic degeneration, was associated with deficits in NREM fast sleep spindle expression over frontal cortex. Furthermore, sleep spindle expression over the same EEG derivations was directly associated with deficits in overnight sleep-dependent episodic memory retention, potentially due to the effects of tau phosphorylation and synaptic degeneration on sleep spindle mechanisms supporting memory-relevant neuroplasticity at the synapse. These findings implicate age-related increases in CNS inflammation and microglial activation as potential early facilitators of tau phosphorylation and neurodegenerative processes reducing the expression of neuroplastic events during sleep that support memory consolidation. CNS inflammaging thus represents a novel, preclinical candidate mechanism that may link aging and AD to memory impairment through its impact on fast sleep spindle expression.

Prior studies have demonstrated links between chronic peripheral inflammation and sleep quality [10, 12, 78, 79]. A meta-analysis of over 70 studies demonstrated that self-reported sleep disturbance, shorter sleep duration, and excessively long sleep duration were associated with increased peripheral C-reactive protein (CRP) and/or interleukin-6 (IL-6) levels [12]. Studies using objective sleep measures showed similar findings, with lower sleep efficiency, lower percent NREM sleep time, severe sleep apnea symptoms, short sleep duration, and higher waking after sleep onset duration all associated with higher plasma IL-6 and/or CRP levels [10, 80]. Experimental sleep deprivation and restriction also lead to increased levels of IL-6, CRP, tumor necrosis factor-α (TNF-α), and nuclear factor κB (NF-κB) [81–83]. Conversely, sleep architecture is disrupted in individuals with chronic inflammatory diseases, thus indicating that these associations may be bidirectional [12]. This potential vicious cycle could be relevant for cognitive aging, as reduced sleep quality and chronic low-grade inflammation have been independently observed with increasing age and hypothesized to contribute to age-related neurological diseases [1, 4, 5, 37]. Recent studies indicate that inflammatory markers such as YKL-40 are associated with reduced slow wave sleep and poor sleep quality in Aβ positive older adults and patients with AD [78, 79]. Despite these findings, there remains a paucity of information regarding whether CNS inflammation is associated with sleep deficits in the absence of Aβ positivity. It also remains unknown whether CNS inflammation is associated with deficits in the local expression of neuroplasticity-relevant fast frequency sleep spindle oscillations observed in aging and AD, and whether there are functional consequences of this relationship.

Our findings address these knowledge gaps in several important ways. First, we report that CSF markers of inflammation (i.e. of astrocyte and microglia activation) were associated with sleep spindle deficits. Moreover, these deficits were local and EEG frequency-specific, with glial activation markers being more specifically associated with NREM sleep spindle-related brain activity at faster frequencies (i.e. 13–<16 Hz vs 11–<13 Hz) over frontal EEG derivations. These associations were also specific to the form of inflammation, with parallelized serial mediation models indicating that NREM sleep spindle-related activity was related to markers of microglial activation but not astrocytic activation. Finally, increased levels of glial activation markers statistically mediated the effects of age on local NREM sleep spindle expression, and these faster frequency sleep spindle deficits were directly related to sleep-dependent memory impairment.

Faster frequency sleep spindles, relative to those of slower frequencies, are more vulnerable to both aging and AD [11, 30]. This is noteworthy given that both our prior work and the findings in the current report demonstrate that deficits in faster frequency sleep spindles contribute to age-related memory deficits [26, 27]. Collectively, these findings identify CNS inflammation as a potential novel contributing factor to age-related deficits in sleep spindles that support neuroplasticity and long-term memory retention. CNS inflammation, in contrast to neurodegeneration, may thus be an early and targetable mechanism contributing to sleep-related memory decline in later life.

Sleep spindle deficits have been reported in people with MCI and AD relative to healthy older adults [11, 29, 31], and the magnitude of these deficits is associated with CSF tau levels even in cognitively unimpaired older adults [13]. Our findings are consistent with these studies, with tau protein levels mediating the effects of age, YKL-40, and soluble TREM2 levels on NREM fast sleep spindle expression. Moreover, these mediations were stronger with phosphorylated tau than total tau, suggesting that inflammation-mediated sleep spindle disruption in older adults may result specifically from the phosphorylation of tau. However, the topographic pattern of sleep spindle deficits in MCI and AD is distinct from that observed in normal aging [4, 5, 11, 30], and the peak of the topographic pattern of associations between age, inflammation, tau proteins, and neuronal integrity in the current report more closely resembled our prior findings in the context of aging, i.e. frontal loss in aging versus parietal in AD [26, 27, 30], though parietal fast sleep spindle deficits were also observed. Thus, proteins associated with CNS inflammation and tau phosphorylation may be critically involved in early age-related sleep changes prior to the onset of tau pathological deposition or neurodegenerative disease.

Though amyloid deposition is thought to be an initial driver of the cortical spread of tau pathology [84, 85], tau protein levels in the current study were below pathological thresholds and were significantly associated with age but not with CSF $A\beta_{42/40}$ levels, likely due to the overall normal amyloid levels in study participants. The topographic pattern of associations between all fast sleep spindle measures and inflammation and phosphorylated tau also differed from those associated with CSF $A\beta_{42/40}$ levels in the current study, with $A\beta_{42/40}$ being more strongly associated with anterior expression of slow sleep spindles. Similar to AD, chronic low grade inflammation is common in normal aging [37]. A recent study in humans examining plasma and CSF measures of 73 inflammatory proteins demonstrated that age was associated with an elevated inflammatory profile in Aβ-negative, cognitively unimpaired older adults, including in proteins associated with inflammatory pathways driving the response to cytokine stimulus, the inflammatory response, and chemotaxis [86]. The degree to which these inflammatory markers were elevated was associated with CSF $A\beta_{42}$, p-tau, t-tau, and cognitive decline as measured by the Clinical Dementia Rating scale sum of boxes [86]. These findings coupled with the findings from our study indicate that aging is associated with inflammation, and the degree of increased inflammation is associated with AD biomarkers and local deficits in sleep spindle expression even prior to Aβ plaque positivity. Beyond phosphorylated tau, CSF measures of synaptic integrity (α-synuclein) also mediated the effects of inflammation on sleep spindle expression. In fact, the most consistently observed indirect effect across sleep spindle measures was through associations between microglial activation and α-synuclein. Thus, these sleep spindle deficits may be a more general marker of memory deficits resulting from synaptic dysfunction regardless of the cause. Sleep spindle-dependent cognitive deficits have been observed across a wide range of neuropsychiatric disorders associated with synaptic dysfunction, including schizophrenia [87], epilepsy [88], attention deficit hyperactivity disorder [89], MCI [90], and Alzheimer's disease [29]. Moreover, sleep spindle deficits in Parkinson's disease predicts the onset of dementia [91]. It is therefore possible that biological processes associated with aging may trigger inflammatory processes within the brain that result in hyperphosphorylation of tau, synaptic degeneration, and sleep spindle-dependent memory deficits that set the stage for either AD pathogenesis or increased vulnerability to AD pathogenesis due to synaptic loss. Another possibility is that tau phosphorylation and synaptic loss contribute specifically to deficits in sleep-dependent memory processing observed in aging, MCI, and AD through their impact on fast sleep spindle expression. While much of the literature has focused on the role of slow wave deficits in impaired sleep-dependent memory consolidation in older adults, MCI patients, and patients with dementia [4, 5], a recent study showed that deficits in sleep spindle measures were associated with impaired sleep-dependent memory in MCI patients [90], and enhancing slow wave-sleep spindle coupling improved sleep-dependent episodic memory in older adults and MCI patients [35, 36, 92]. Our findings build on this work to identify candidate mechanisms for sleep spindle-dependent memory impairment in older adults at risk for AD.

The effect of microglial activation on production of phosphorylated tau is a recognized pathway triggering early stages of AD pathophysiological progression [38, 39]. Though the existing literature has focused on the triggering effect of Aβ pathology on microglia that then fosters pathological accumulation of tau and neurodegeneration [38, 39], numerous studies implementing rodent tauopathy models support direct links between microglial function and tau pathophysiology even in the absence of Aβ [93–97]. One mechanism that contributes to this relationship between microglial dysfunction and tau pathophysiology, neurodegeneration, and cognitive impairment is TREM2. TREM2 expression is specific to microglia [98], and mutations in the gene coding TREM2 increases AD risk [99]. Higher sTREM2 levels in CSF is associated with tau proteins and neurodegeneration in humans,[100] and tau-expressing TREM2 knockout mice show lower levels of microglial activation and reduced hippocampal atrophy [95]. Thus, microglial dysfunction, potentially operating through a TREM2 mechanism, may foster the production and phosphorylation of tau and related synaptic degeneration that underlies the deficits in fast sleep spindle expression observed in the current study. Supporting this possibility, CSF sTREM2 levels mediated the effects of age on fast sleep spindle expression in the current study and were associated with tau and α-synuclein levels. Our findings suggest that tau-related fast sleep spindle deficits may be among the earliest sleep-related deficits observed in AD, since participants were relatively young (~62% between 48 and 60 years old), cognitively unimpaired, and largely amyloid and tau negative based on established CSF thresholds [67].

A recent report demonstrated a key role for NfL in reduced slow wave sleep in AD patients [79], a brain state rich in slow waves and sleep spindles. Our findings are consistent in that NfL levels were negatively associated with both global NREM

sleep spindle expression and delta activity. Nevertheless, these findings were unexpected given that the subject cohort was negative for Aβ and tau pathology based on established CSF thresholds [67], which is thought to precede the widespread NfL-associated neurodegeneration observed in later AD stages [84]. However, a recent report has shown that NfL is also associated with age-related brain atrophy in a cognitively unimpaired older adult cohort absent of neurological injury or neurodegenerative disease.[101] Cortical brain atrophy has been associated with both reduced SWA and sleep spindle deficits in cognitively unimpaired older adults in other studies.[9, 15, 27, 102] Collectively, these findings suggest that the reduced delta activity and sleep spindle expression deficits associated with NfL in the current study may represent age-related brain atrophy impacting sleep oscillation expression. It is also important to note, however, that NfL was not associated only with sleep spindle expression and delta activity deficits, as associations with NfL were present across almost all frequency bands. This indicates that NfL may be more tied to loss of global power across frequencies, potentially independent of sleep state, due solely to the effects of global neuronal loss on absolute amplitude of neural activity. In further support of this possibility, fast sigma oscillatory activity was not significantly associated with NfL levels, and the aperiodic power offset did show a significant association with NfL.

While these findings identify candidate mechanistic links among CNS inflammation, AD biomarkers, and sleep-related memory processing, this study has some limitations. First, these cross-sectional findings are associational and do not prove causal links between variables. A combination of targeted longitudinal and experimental manipulation studies will be needed to evaluate the causal nature of these reported associations. Second, the study was not powered to address potential effects of sex as a biological variable in moderating the reported effects, which will be critical as sex impacts microglial function and CNS inflammation [103], AD biomarkers [104], global and local sleep expression [5, 105], and potentially their interactive impact on cognition [106, 107]. Larger studies will be needed to examine how sex impacts these relationships. Another important limitation regards the lack of Aβ plaque and neurofibrillary tangle positivity among the study cohort. Even though nearly 80% of the cohort has parental history of AD, which increases risk for AD [108], it remains uncertain whether or not the study participants are on the trajectory toward the development of AD. It is therefore unclear whether these associations are driven by processes associated with age or preclinical stages AD pathogenesis. While these findings are important regardless of the root cause, future studies will need to examine the evolution of these relationships across preclinical and clinical stages of AD. The lack of neuroimaging of neurodegeneration and pathology markers also precludes examining the brain circuit specificity of the reported effects, though the molecular specificity of AD fluid biomarkers is an important advantage of the current study. Finally, the study focused on markers of CNS inflammation and markers of peripheral inflammation were not assessed. The importance of this was recently highlighted in a proteome study that demonstrated that inflammatory pathways measured in plasma and CSF may be differentially associated with AD biomarkers, neurodegeneration, and cognitive decline [86]. Future studies combining both measures will thus be critical to elucidate how the interactions between central and peripheral inflammation impacts the relationship between AD biomarkers, local sleep expression, and related cognitive functions.

In conclusion, these findings demonstrate that markers of CNS inflammation are associated with AD-related proteins and neurodegenerative processes that in turn were associated with local expression of sleep spindles and sleep-dependent memory retention in cognitively unimpaired older adults at risk for AD. They support findings from rodent models implicating microglia, possibly through TREM2-mediated pathways, in early expression of AD pathophysiology [16, 95, 100, 109], and associate these markers with sleep spindle expression deficits and associated sleep-dependent memory deficits in humans enriched for AD risk. Future studies will need to build on this framework to better understand how CNS inflammation is mechanistically linked to AD-related proteins and related brain pathology, neuronal integrity, and local deficits in sleep oscillations supporting neuroplasticity. Longitudinal studies are required to characterize the temporal relationships between CNS inflammation, AD-related proteins, brain pathology, and neuronal integrity. Intervention studies will be needed to determine whether targeting microglia activation, or other mechanisms of CNS inflammation, could minimize fast sleep spindle deficits, sleep-dependent cognitive impairment, and dementia risk. Lastly, studies of populations at risk for AD dementia that examine sleep spindle deficits should also examine CNS markers of inflammation, which may precede the onset of clinically significant AD pathology and synaptic loss [16, 95, 96, 100, 109, 110].

Supplementary Material

Supplementary material is available at *SLEEP* online.

Acknowledgments

We would like to thank participants and staff of the Wisconsin ADRC and Wisconsin Sleep for their contributions to the study, and the laboratory technicians at the Clinical Neurochemistry Laboratory, in Mölndal, Sweden. Without their efforts this research would not be possible. We would also like to thank Drs. Richard Gao and Bradley Voytek for their assistance in implementing the "fitting oscillations and one over f" (FOOOF) signal processing approach to our sleep electroencephalography (EEG) analyses. CSF assays kits were provided by Roche Diagnostics GmbH. This research was supported by grants R56 AG052698, R01 AG027161, R01 AG021155, ADRC P50 AG033514, R01 AG037639, K01 AG068353, and National Research Service Award F31 AG048732 from the National Institute on Aging, and by the Clinical and Translational Science Award (CTSA) program, through the NIH National Center for Advancing Translational Sciences (NCATS), grant UL1TR000427. Dr. Zetterberg is a Wallenberg Scholar supported by grants from the Swedish Research Council (#2018-02532), the European Research Council (#681712), Swedish State Support for Clinical Research (#ALFGBG-720931), the Alzheimer Drug Discovery Foundation (ADDF), USA (#201809-2016862), the AD Strategic Fund and the Alzheimer's Association (#ADSF-21-831376-C, #ADSF-21-831381-C and #ADSF-21-831377-C), the Olav Thon Foundation, the Erling-Persson Family Foundation, Stiftelsen för Gamla Tjänarinnor, Hjärnfonden, Sweden (#FO2019-0228), the European Union's Horizon 2020 research and innovation

programme under the Marie Skłodowska-Curie grant agreement No 860197 (MIRIADE), and the UK Dementia Research Institute at UCL. Dr. Blennow is supported by the Swedish Research Council (#2017-00915), the Swedish Alzheimer Foundation (#AF-742881), Hjärnfonden, Sweden (#FO2017-0243), and the Swedish state under the agreement between the Swedish government and the County Councils, the ALF-agreement (#ALFGBG-715986). The content is solely the responsibility of the authors and does not necessarily represent the official views of the NIH. COBAS, COBAS E, and ELECSYS are trademarks of Roche.

Author Contributions

B.A.M. analyzed the data and wrote the manuscript. A.D., K.K.L., M.G.C., and I.Y.C. aided in analyzing the data and writing the manuscript. K.E.S. conducted the experiments, overseeing sleep and memory data collection as part of her dissertation, and aided in data analysis and writing the manuscript. D.B. aided in data analytic tool development, data analysis, and manuscript preparation. B.A.R. aided in sleep study data collection, provided data analytic tools, and aided in manuscript preparation. M.H. aided collection and analysis of demographic, neuropsychological, and CSF data, and edited the manuscript. I.S., G.K., H.Z., and K.B. oversaw CSF data analysis and edited the manuscript. C.M.C., O.C.O., S.A., and S.C.J. aided data collection, neuropsychological screening, and manuscript preparation. B.B.B. aided study design, provided the subject pool, and aided in data analysis and manuscript preparation. Lastly, R.M.B. designed the study, oversaw clinical sleep screening procedures, aided in data collection and analysis, and aided writing the manuscript.

Disclosure statement

Financial disclosure: Dr. Mander has served as a consultant for Eisai Co., Ltd. Dr. Benca has served as a consultant for Eisai, Genomind, Idorsia, Jazz, Merck, and Sunovion. Dr. Zetterberg has served at scientific advisory boards for Eisai, Denali, Roche Diagnostics, Wave, Samumed, Siemens Healthineers, Pinteon Therapeutics, Nervgen, AZTherapies and CogRx. Dr. Blennow has served as a consultant, at advisory boards, or at data monitoring committees for Abcam, Axon, Biogen, JOMDD/Shimadzu. Julius Clinical, Lilly, MagQu, Novartis, Roche Diagnostics, and Siemens Healthineers. Dr. Riedner has several patents related to sleep technology jointly held by the Wisconsin Alumni Research Foundation and Philips Healthcare, and in addition to grant support, has given several lectures sponsored by Philips Healthcare. Dr. Suridjan is a shareholder of Roche Diagnostics International Ltd.

Non-financial disclosure: Dr. Zetterberg has given lectures in symposia sponsored by Cellectricon, Fujirebio, Alzecure and Biogen, and is a co-founder of Brain Biomarker Solutions in Gothenburg AB (BBS), which is a part of the GU Ventures Incubator Program. Dr. Blenow is a co-founder of Brain Biomarker Solutions in Gothenburg AB (BBS), which is a part of the GU Ventures Incubator Program. Dr. Kollmorgen is a full-time employee of Roche Diagnostics GmbH. Dr. Suridjan is a full-time employee of Roche Diagnostics International Ltd.

References

1. Deleidi M, *et al*. Immune aging, dysmetabolism, and inflammation in neurological diseases. *Front Neurosci*. 2015;**9**:172. doi:10.3389/fnins.2015.00172.
2. Jagust W. Vulnerable neural systems and the borderland of brain aging and neurodegeneration. *Neuron*. 2013;**77**(2):219–234. doi:10.1016/j.neuron.2013.01.002.
3. Leal SL, *et al*. Perturbations of neural circuitry in aging, mild cognitive impairment, and Alzheimer's disease. *Ageing Res Rev*. 2013;**12**(3):823–831. doi:10.1016/j.arr.2013.01.006.
4. Mander BA. Local sleep and Alzheimer's disease pathophysiology. *Front Neurosci*. 2020;**14**:1008. doi:10.3389/fnins.2020.525970.
5. Mander BA, *et al*. Sleep and human aging. *Neuron* 2017;**94**(1):19–36. doi:10.1016/j.neuron.2017.02.004.
6. Irwin MR, *et al*. Implications of sleep disturbance and inflammation for Alzheimer's disease dementia. *Lancet Neurol*. 2019;**18**:296–306. doi:10.1016/S1474-4422(18)30450-2.
7. Tangestani Fard M, *et al*. A review and hypothesized model of the mechanisms that underpin the relationship between inflammation and cognition in the elderly. *Front Aging Neurosci*. 2019;**11**:56. doi:10.3389/fnagi.2019.00056.
8. Djonlagic I, *et al*. Macro and micro sleep architecture and cognitive performance in older adults. *Nat Hum Behav*. 2021;**5**(1):123–145. doi:10.1038/s41562-020-00964-y.
9. Fogel S, *et al*. Sleep spindles: a physiological marker of age-related changes in gray matter in brain regions supporting motor skill memory consolidation. *Neurobiol Aging*. 2017;**49**:154164. doi:10.1016/j.neurobiolaging.2016.10.009.
10. Friedman EM, *et al*. Social relationships, sleep quality, and interleukin-6 in aging women. *Proc Natl Acad Sci USA*. 2005;**102**(51):18757–18762. doi:10.1073/pnas.0509281102.
11. Gorgoni M, *et al*. Parietal fast sleep spindle density decrease in Alzheimer's disease and amnesic mild cognitive impairment. *Neural Plast*. 2016;**2016**:8376108. doi:10.1155/2016/8376108.
12. Irwin MR, *et al*. Sleep disturbance, sleep duration, and inflammation: a systematic review and meta-analysis of cohort studies and experimental sleep deprivation. *Biol Psychiatry*. 2016;**80**(1):40–52. doi:10.1016/j.biopsych.2015.05.014.
13. Kam K, *et al*. Sleep oscillation-specific associations with Alzheimer's disease CSF biomarkers: novel roles for sleep spindles and tau. *Mol Neurodegener*. 2019;**14**(1):10. doi:10.1186/s13024-019-0309-5.
14. Mander BA, *et al*. beta-amyloid disrupts human NREM slow waves and related hippocampus-dependent memory consolidation. *Nat Neurosci*. 2015;**18**(7):1051–1057. doi:10.1038/nn.4035.
15. Mander BA, *et al*. Prefrontal atrophy, disrupted NREM slow waves and impaired hippocampal-dependent memory in aging. *Nat Neurosci*. 2013;**16**(3):357–364.
16. Spangenberg EE, *et al*. Eliminating microglia in Alzheimer's mice prevents neuronal loss without modulating amyloid-beta pathology. *Brain*. 2016;**139**(Pt 4):1265–1281. doi:10.1093/brain/aww016.
17. Sprecher KE, *et al*. Poor sleep is associated with CSF biomarkers of amyloid pathology in cognitively normal adults. *Neurology*. 2017;**89**(5):445–453. doi:10.1212/Wnl.0000000000004171.
18. Winer JR, *et al*. Sleep as a potential biomarker of tau and beta-amyloid burden in the human brain. *J Neurosci*. 2019;**39**(32):6315–6324. doi:10.1523/JNEUROSCI.0503-19.2019.
19. Frank MG, *et al*. mRNA up-regulation of MHC II and pivotal pro-inflammatory genes in normal brain aging. *Neurobiol Aging*. 2006;**27**(5):717–722. doi:10.1016/j.neurobiolaging.2005.03.013.

20. Gais S, *et al*. Learning-dependent increases in sleep spindle density. *J Neurosci*. 2002;**22**(15):6830–6834. doi:10.1523/JNEUROSCI.22-15-06830.2002.
21. Latchoumane CV, *et al*. Thalamic spindles promote memory formation during sleep through triple phase-locking of cortical, thalamic, and hippocampal rhythms. *Neuron* 2017;**95**(2):424–435. doi:10.1016/j.neuron.2017.06.025.
22. Lustenberger C, *et al*. Feedback-controlled transcranial alternating current stimulation reveals a functional role of sleep spindles in motor memory consolidation. *Curr Biol*. 2016;**26**(16):2127–2136. doi:10.1016/j.cub.2016.06.044.
23. Mander BA, *et al*. Wake deterioration and sleep restoration of human learning. *Curr Biol*. 2011;**21**(5):R183–R184. doi:10.1016/j.cub.2011.01.019.
24. Rosanova M, *et al*. Pattern-specific associative long-term potentiation induced by a sleep spindle-related spike train. *J Neurosci*. 2005;**25**(41):9398–9405. doi:10.1523/Jneurosci.2149-05.2005.
25. Steriade M. Grouping of brain rhythms in corticothalamic systems. *Neuroscience* 2006;**137**(4):1087–1106. doi:10.1016/j.neuroscience.2005.10.029.
26. Mander BA, *et al*. Impaired prefrontal sleep spindle regulation of hippocampal-dependent learning in older adults. *Cereb Cortex*. 2014;**24**(12):3301–3309. doi:10.1093/cercor/bht188.
27. Mander BA, *et al*. White matter structure in older adults moderates the benefit of sleep spindles on motor memory consolidation. *J Neurosci*. 2017;**37**(48):11675–11687. doi:10.1523/JNEUROSCI.3033-16.2017.
28. Martin N, *et al*. Topography of age-related changes in sleep spindles. *Neurobiol Aging*. 2013;**34**(2):468–476. doi:10.1016/j.neurobiolaging.2012.05.020.
29. Rauchs G, *et al*. Is there a link between sleep changes and memory in Alzheimer's disease? *Neuroreport* 2008;**19**(11):1159–1162. doi:10.1097/WNR.0b013e32830867c4.
30. Sprecher KE, *et al*. High resolution topography of age-related changes in non-rapid eye movement sleep electroencephalography. *PLos One* 2016;**11**(2):e0149770. doi:10.1371/journal.pone.0149770.
31. Westerberg CE, *et al*. Concurrent impairments in sleep and memory in Amnestic mild cognitive impairment. *J Int Neuropsychol Soc*. 2012;**18**(3):490–500. doi:10.1017/S135561771200001X.
32. Holth JK, *et al*. Altered sleep and EEG power in the P301S Tau transgenic mouse model. *Ann Clin Transl Neurol*. 2017;**4**(3):180–190. doi:10.1002/acn3.390.
33. Fogel SM, *et al*. fMRI and sleep correlates of the age-related impairment in motor memory consolidation. *Hum Brain Mapp*. 2014;**35**:3625–3645. doi:10.1002/hbm.22426.
34. Ladenbauer J, *et al*. Promoting sleep oscillations and their functional coupling by transcranial stimulation enhances memory consolidation in mild cognitive impairment. *J Neurosci*. 2017;**37**(30):7111–7124. doi:10.1523/JNEUROSCI.0260-17.2017.
35. Papalambros NA, *et al*. Acoustic enhancement of sleep slow oscillations and concomitant memory improvement in older adults. *Front Hum Neurosci*. 2017;**11**:109. doi:10.3389/fnhum.2017.00109.
36. Papalambros NA, *et al*. Acoustic enhancement of sleep slow oscillations in mild cognitive impairment. *Ann Clin Transl Neurol*. 2019;**6**(7):1191–1201. doi:10.1002/acn3.796.
37. Ferrucci L, *et al*. Inflammageing: chronic inflammation in ageing, cardiovascular disease, and frailty. *Nat Rev Cardiol*. 2018;**15**(9):505–522. doi:10.1038/s41569-018-0064-2.
38. Heppner FL, *et al*. Immune attack: the role of inflammation in Alzheimer disease. *Nat Rev Neurosci*. 2015;**16**(6):358–372. doi:10.1038/nrn3880.
39. Spangenberg EE, *et al*. Inflammation in Alzheimer's disease: lessons learned from microglia-depletion models. *Brain Behav Immun*. 2017;**61**:1–11. doi:10.1016/j.bbi.2016.07.003.
40. Krstic D, *et al*. Systemic immune challenges trigger and drive Alzheimer-like neuropathology in mice. *J Neuroinflammation*. 2012;**9**:151. doi:10.1186/1742-2094-9-151.
41. Brothers HM, *et al*. Riluzole partially rescues age-associated, but not LPS-induced, loss of glutamate transporters and spatial memory. *J Neuroimmune Pharmacol*. 2013;**8**(5):1098–1105. doi:10.1007/s11481-013-9476-2.
42. Barrientos RM, *et al*. Memory impairments in healthy aging: role of aging-induced microglial sensitization. *Aging Dis*. 2010;**1**(3):212–231. PMID: 21132050; PMCID: PMC2995216.
43. Elmore MRP, *et al*. Replacement of microglia in the aged brain reverses cognitive, synaptic, and neuronal deficits in mice. *Aging Cell*. 2018;**17**(6):e12832. doi:10.1111/acel.12832.
44. Musella A, *et al*. Interplay between age and neuroinflammation in multiple sclerosis: effects on motor and cognitive functions. *Front Aging Neurosci*. 2018;**10**:238. doi:10.3389/fnagi.2018.00238.
45. Salazar AM, *et al*. Alterations of GABA B receptors in the APP/PS1 mouse model of Alzheimer's disease. *Neurobiol Aging*. 2021;**97**:129–143. doi:10.1016/j.neurobiolaging.2020.10.013.
46. Weintraub S, *et al*. Version 3 of the Alzheimer Disease Centers' neuropsychological test battery in the uniform data set (UDS). *Alzheimer Dis Assoc Disord*. 2018;**32**(1):10–17. doi:10.1097/WAD.0000000000000223.
47. Albert MS, *et al*. The diagnosis of mild cognitive impairment due to Alzheimer's disease: recommendations from the National Institute on Aging-Alzheimer's Association workgroups on diagnostic guidelines for Alzheimer's disease. *Alzheimers Dement*. 2011;**7**(3):270–279. doi:10.1016/j.jalz.2011.03.008.
48. McKhann GM, *et al*. The diagnosis of dementia due to Alzheimer's disease: recommendations from the National Institute on Aging-Alzheimer's Association workgroups on diagnostic guidelines for Alzheimer's disease. *Alzheimers Dement*. 2011;**7**(3):263–269. doi:10.1016/j.jalz.2011.03.005.
49. Berry RB, *et al*. Rules for scoring respiratory events in sleep: update of the 2007 AASM manual for the scoring of sleep and associated events. Deliberations of the Sleep Apnea Definitions Task Force of the American Academy of Sleep Medicine. *J Clin Sleep Med*. 2012;**8**(5):597–619. doi:10.5664/jcsm.2172.
50. Silber MH, *et al*. The visual scoring of sleep in adults. *J Clin Sleep Med*. 2007;**3**(2):121–131. PMID: 17557422.
51. Jones SG, *et al*. Regional reductions in sleep electroencephalography power in obstructive sleep apnea: a high-density EEG study. *Sleep*. 2014;**37**(2):399–407. doi:10.5665/sleep.3424.
52. Plante DT, *et al*. Altered slow wave activity in major depressive disorder with hypersomnia: a high density EEG pilot study. *Psychiatry Res*. 2012;**201**(3):240–244. doi:10.1016/j.pscychresns.2012.03.001.
53. Riedner BA, *et al*. Regional patterns of elevated alpha and high-frequency electroencephalographic activity during nonrapid eye movement sleep in chronic insomnia: a pilot study. *Sleep*. 2016;**39**(4):801–812. doi:10.5665/sleep.5632.
54. Riedner BA, *et al*. Sleep homeostasis and cortical synchronization: III. A high-density EEG study of sleep slow waves in humans. *Sleep*. 2007;**30**(12):1643–1657. doi:10.1093/sleep/30.12.1643.

55. Ferree TC. Spherical splines and average referencing in scalp electroencephalography. *Brain Topogr*. 2006;**19**(1-2):43–52. doi:10.1007/s10548-006-0011-0.
56. Perrin F, *et al*. Spherical splines for scalp potential and current density mapping. *Electroencephalogr Clin Neurophysiol*. 1989;**72**(2):184–187. doi:10.1016/0013-4694(89)90180-6.
57. Babadi B, *et al*. A review of multitaper spectral analysis. *IEEE Trans Biomed Eng*. 2014;**61**(5):1555–1564. doi:10.1109/TBME.2014.2311996.
58. Mitra P, Bokil H. *Observed Brain Dynamics*. New York, NY: Oxford University Press; 2008.
59. Prerau MJ, *et al*. Sleep neurophysiological dynamics through the lens of multitaper spectral analysis. *Physiology (Bethesda)*. 2017;**32**(1):60–92. doi:10.1152/physiol.00062.2015.
60. Donoghue T, *et al*. Parameterizing neural power spectra into periodic and aperiodic components. *Nat Neurosci*. 2020;**23**(12):1655–1665. doi:10.1038/s41593-020-00744-x.
61. Donoghue T, *et al*. Electrophysiological frequency band ratio measures conflate periodic and aperiodic neural activity. *eNeuro*. 2020;**7**(6):ENEURO.0192–20. doi:10.1523/ENEURO.0192-20.2020.
62. Miller KJ, *et al*. Power-law scaling in the brain surface electric potential. *PLoS Comput Biol*. 2009;**5**(12):e1000609. doi:10.1371/journal.pcbi.1000609.
63. Meisel C, *et al*. The interplay between long- and short-range temporal correlations shapes cortex dynamics across vigilance states. *J Neurosci*. 2017;**37**(42):10114–10124. doi:10.1523/JNEUROSCI.0448-17.2017.
64. Gao R, *et al*. Inferring synaptic excitation/inhibition balance from field potentials. *Neuroimage* 2017;**158**:70–78. doi:10.1016/j.neuroimage.2017.06.078.
65. Manning JR, *et al*. Broadband shifts in local field potential power spectra are correlated with single-neuron spiking in humans. *J Neurosci*. 2009;**29**(43):13613–13620. doi:10.1523/JNEUROSCI.2041-09.2009.
66. Lacourse K, *et al*. A sleep spindle detection algorithm that emulates human expert spindle scoring. *J Neurosci Methods*. 2019;**316**:3–11. doi:10.1016/j.jneumeth.2018.08.014.
67. Van Hulle C, *et al*. An examination of a novel multipanel of CSF biomarkers in the Alzheimer's disease clinical and pathological continuum. *Alzheimers Dement*. 2020. doi:10.1002/alz.12204.
68. Mattsson-Carlgren N, *et al*. Aβ deposition is associated with increases in soluble and phosphorylated tau that precede a positive Tau PET in Alzheimer's disease. *Sci Adv*. 2020;**6**(16):eaaz2387. doi:10.1126/sciadv.aaz2387.
69. Marshall L, *et al*. Boosting slow oscillations during sleep potentiates memory. *Nature*. 2006;**444**(7119):610–613. doi:10.1038/nature05278.
70. Marshall L, *et al*. Transcranial direct current stimulation during sleep improves declarative memory. *J Neurosci*. 2004;**24**(44):9985–9992. doi:10.1523/JNEUROSCI.2725-04.2004.
71. Plihal W, *et al*. Effects of early and late nocturnal sleep on declarative and procedural memory. *J Cogn Neurosci*. 1997;**9**(4):534–547. doi:10.1162/jocn.1997.9.4.534.
72. Mensen A, *et al*. Advanced EEG analysis using threshold-free cluster-enhancement and non-parametric statistics. *Neuroimage*. 2013;**67**:111–118. doi:10.1016/j.neuroimage.2012.10.027.
73. Plante DT, *et al*. Establishing the objective sleep phenotype in hypersomnolence disorder with and without comorbid major depression. *Sleep*. 2019;**42**(6). doi: 10.1093/sleep/zsz060.
74. Smith SM, *et al*. Threshold-free cluster enhancement: addressing problems of smoothing, threshold dependence and localisation in cluster inference. *Neuroimage*. 2009;**44**(1):83–98. doi:10.1016/j.neuroimage.2008.03.061.
75. Efron B. Better bootstrap confidence intervals. *J Am Stat Assoc*. 1987;**82**(397):171–185. doi:10.2307/2289144.
76. Hayes AF. *Introduction to Mediation, Moderation, and Conditional Process Analysis. A Regression-Based Approach*. 2nd ed. New York City, NY: The Guilford Press; 2018. doi:10.1093/sleep/zsaa147.
77. Preacher KJ, *et al*. SPSS and SAS procedures for estimating indirect effects in simple mediation models. *Behav Res Methods Instrum Comput*. 2004;**36**(4):717–731. doi:10.3758/bf03206553.
78. Fjell AM, *et al*. Neuroinflammation and Tau interact with amyloid in predicting sleep problems in aging independently of atrophy. *Cereb Cortex*. 2018;**28**(8):2775–2785. doi:10.1093/cercor/bhx157.
79. Targa A, *et al*. Decrease in sleep depth is associated with higher cerebrospinal fluid neurofilament light levels in patients with Alzheimer's disease. *Sleep*. 2021;**44**(2). doi:10.1093/sleep/zsaa147.
80. Smagula SF, *et al*. Actigraphy- and polysomnography-measured sleep disturbances, inflammation, and mortality among older men. *Psychosom Med*. 2016;**78**(6):686–696. doi:10.1097/PSY.0000000000000312.
81. Irwin MR, *et al*. Sleep loss activates cellular inflammatory signaling. *Biol Psychiatry*. 2008;**64**(6):538–540. doi:10.1016/j.biopsych.2008.05.004.
82. Meier-Ewert HK, *et al*. Effect of sleep loss on C-reactive protein, an inflammatory marker of cardiovascular risk. *J Am Coll Cardiol*. 2004;**43**(4):678–683. doi:10.1016/j.jacc.2003.07.050.
83. Shearer WT, *et al*. Soluble TNF-alpha receptor 1 and IL-6 plasma levels in humans subjected to the sleep deprivation model of spaceflight. *J Allergy Clin Immunol*. 2001;**107**(1):165–170. doi:10.1067/mai.2001.112270.
84. Jack CR, *et al*. Tracking pathophysiological processes in Alzheimer's disease: an updated hypothetical model of dynamic biomarkers. *Lancet Neurol*. 2013;**12**(2):207–216. doi:10.1038/s41583-018-0067-3.
85. Jagust W. Imaging the evolution and pathophysiology of Alzheimer disease. *Nat Rev Neurosci*. 2018;**19**(11):687–700.
86. Cullen NC, *et al*. Accelerated inflammatory aging in Alzheimer's disease and its relation to amyloid, tau, and cognition. *Sci Rep*. 2021;**11**(1):1965. doi:10.1038/s41598-021-81705-7.
87. Manoach DS, *et al*. Abnormal sleep spindles, memory consolidation, and schizophrenia. *Annu Rev Clin Psychol*. 2019;**15**:451–479. doi:10.1146/annurev-clinpsy-050718-095754.
88. Kramer MA, *et al*. Focal sleep spindle deficits reveal focal thalamocortical dysfunction and predict cognitive deficits in sleep activated developmental epilepsy. *J Neurosci*. 2021;**41**(8):1816–1829. doi:10.1523/JNEUROSCI.2009-20.2020.
89. Merikanto I, *et al*. ADHD symptoms are associated with decreased activity of fast sleep spindles and poorer procedural overnight learning during adolescence. *Neurobiol Learn Mem*. 2019;**157**:106–113. doi:10.1016/j.nlm.2018.12.004.
90. Lam A, *et al*. Sleep-dependent memory in older people with and without MCI: the relevance of sleep microarchitecture, OSA, hippocampal subfields, and episodic memory. *Cereb Cortex*. 2021;**31**(6):2993–3005. doi:10.1093/cercor/bhaa406.
91. Latreille V, *et al*. Sleep spindles in Parkinson's disease may predict the development of dementia. *Neurobiol Aging*. 2015;**36**(2):1083–1090. doi:10.1016/j.neurobiolaging.2014.09.009.
92. Westerberg CE, *et al*. Memory improvement via slow-oscillatory stimulation during sleep in older adults.

Neurobiol Aging. 2015;**36**(9):2577–2586. doi:10.1016/j.neurobiolaging.2015.05.014.
93. Asai H, *et al*. Depletion of microglia and inhibition of exosome synthesis halt tau propagation. *Nat Neurosci*. 2015;**18**(11):1584–1593. doi:10.1038/nn.4132.
94. Bussian TJ, *et al*. Clearance of senescent glial cells prevents tau-dependent pathology and cognitive decline. *Nature*. 2018;**562**(7728):578–582. doi:10.1038/s41586-018-0543-y.
95. Leyns CEG, *et al*. TREM2 deficiency attenuates neuroinflammation and protects against neurodegeneration in a mouse model of tauopathy. *Proc Natl Acad Sci USA*. 2017;**114**(43):11524–11529. doi:10.1073/pnas.1710311114.
96. Maphis N, *et al*. Reactive microglia drive tau pathology and contribute to the spreading of pathological tau in the brain. *Brain*. 2015;**138**(Pt 6):1738–1755. doi:10.1093/brain/awv081.
97. Yoshiyama Y, *et al*. Synapse loss and microglial activation precede tangles in a P301S tauopathy mouse model. *Neuron*. 2007;**53**(3):337–351. doi:10.1016/j.neuron.2007.01.010.
98. Ulrich JD, *et al*. Elucidating the role of TREM2 in Alzheimer's disease. *Neuron*. 2017;**94**(2):237–248. doi:10.1016/j.neuron.2017.02.042.
99. Jonsson T, *et al*. Variant of TREM2 associated with the risk of Alzheimer's disease. *N Engl J Med*. 2013;**368**(2):107–116. doi:10.1056/NEJMoa1211103.
100. Suarez-Calvet M, *et al*. Early increase of CSF sTREM2 in Alzheimer's disease is associated with tau related-neurodegeneration but not with amyloid-beta pathology. *Mol Neurodegener*. 2019;**14**(1):1. doi:10.1186/s13024-018-0301-5.
101. Khalil M, *et al*. Serum neurofilament light levels in normal aging and their association with morphologic brain changes. *Nat Commun*. 2020;**11**(1):812. doi:10.1038/s41467-020-14612-6.
102. Dube J, *et al*. Cortical thinning explains changes in sleep slow waves during adulthood. *J Neurosci*. 2015;**35**(20):7795–7807. doi:10.1523/JNEUROSCI.3956-14.2015.
103. Hanamsagar R, *et al*. Sex differences in neurodevelopmental and neurodegenerative disorders: Focus on microglial function and neuroinflammation during development. *J Steroid Biochem Mol Biol*. 2016;**160**:127–133. doi:10.1016/j.jsbmb.2015.09.039.
104. Sundermann EE, *et al*. Sex differences in Alzheimer's-related Tau biomarkers and a mediating effect of testosterone. *Biol Sex Differ*. 2020;**11**(1):33. doi:10.1186/s13293-020-00310-x.
105. Huupponen E, *et al*. A study on gender and age differences in sleep spindles. *Neuropsychobiology*. 2002;**45**(2):99–105. doi:10.1159/000048684.
106. Buckley RF, *et al*. Sex differences in the association of global amyloid and regional tau deposition measured by positron emission tomography in clinically normal older adults. *JAMA Neurol*. 2019;**76**(5):542–551. doi:10.1001/jamaneurol.2018.4693.
107. Buckley RF, *et al*. Sex mediates relationships between regional tau pathology and cognitive decline. *Ann Neurol*. 2020;**88**(5):921–932. doi:10.1002/ana.25878.
108. Fratiglioni L, *et al*. Risk factors for late-onset Alzheimer's disease: a population-based, case-control study. *Ann Neurol*. 1993;**33**(3):258–266. doi:10.1002/ana.410330306.